Master's thesis

Generic Radar Model for Automotive Applications

Mario Grgic BSc

Graz University of Technology
Faculty of Electrical Engineering

Institute of Electrical Measurement and Signal Processing [EMT]
and
Institute of Automotive Engineering [FTG]
Member of Frank Stronach Institute

Supervisor: Dipl.-Ing.Dr.techn.Markus Neumayer [EMT]
and
Univ.-Doz.Dipl.-Ing.Dr.techn. Arno Eichberger [FTG]

Graz, 30.09.2015

Contents

Acknowledgement

I am heartily thankful to my supervisor, Markus Neumayer from the Institute of Electrical Measurement and Signal Processing, whose encouragement, guidance and support from the start to the final level enabled me to develop an understanding of the project.

Furthermore I would like to bring my gratitude to Arno Eichberger the head of driver assistance and vehicle dynamics from the Institute of Automotive Engineering who gave me the opportunity to work on this thesis. I also would like to thank Branko Rogic and Zoltan Magosi, for there effort and the cooperation and support.

I would thank all who made this thesis possible.

Statutory Declaration

Ich erkläre an Eides statt, dass ich die vorliegende Arbeit selbstständig verfasst, andere als die angegebenen Quellen/Hilfsmittel nicht benutzt, und die den benutzten Quellen wörtlich und inhaltlich entnommenen Stellen als solche kenntlich gemacht habe.

Graz, am ....
(Unterschrift)

I declare that I have authored this thesis independently, that I have not used other than the declared sources / resources, and that I have explicitly marked all material which has been quoted either literally or by content from the used sources.

....
(date) (signature)

Abstract

Advanced driving assistance systems are gaining more and more importance in modern vehicles. They are used to assist the driver, e.g. in applications like cruise control, but recent development trends even consider, the take over of the vehicle control by the driving assistance system. Such techniques are considered to efficiently avoid or counteract on dangerous situations. Key enabler for such driving assistance systems are sensors, which provide information about the vehicle and the surrounding traffic scenario. For long distance ranging and detection of vehicles/obstacles in front of the own vehicle, radar technology has seen strong developments over the past years and radar sensors have become a standard sensors for many modern vehicles. The development of high level driving assistance systems, which are able to provide correct and reliable performance for complex traffic scenarios, is a demanding problem for control engineers. Simulation is a mandatory tool for the development and testing of this control systems. Subsequently, this simulation tools require realistic sensor models, in order to generate input data for the algorithms to be developed. This thesis presents the development of a generic radar sensor model/simulator. The simulator can be applied in any Matlab/Simulink based driving simulator. Given the driving scenario as input data in front of the vehicle, the model scans the field of view of the sensor, by means of an ray tracing algorithm. Given the sight of the scene computed by the ray tracer, the radar signal is computed by incorporating radar systems specifics, e.g. the antenna pattern, transmitted power, etc. Basic radar signal processing methods then extract generic object information to be used for the following processing unit. The developed radar simulator can be used in real time driving simulators for the development of driving assistance systems, but also for the development of improved radar signal processing techniques.

Kurzfassung

Der Einsatz von Fahrerassistenzsystemen in modernen Fahrzeugen gewinnt immer mehr an Bedeutung. Solche Systeme werden verwendet um den Fahrer zu unterstützen, z.B. in Anwendungen wie dem Tempomat. Neuere Entwicklungen erlauben das Eingreifen in das Fahrgeschehen des Fahrzeuges. Solche Systeme werden deshalb verwendet, um in gefährlichen Situationen gegenzusteuern bzw. solche gänzlich zu vermeiden. Eine Schlüsselrolle bei Fahrerassistenzsystemen nehmen Sensoren ein, welche Information über das Fahrzeug und die Umgebung bereitstellen. Bei der Distanzmessung und Erfassung von Fahrzeugen/Objekten bei großen Reichweiten, ist die Entwicklung von Radarsensoren stetig voran geschritten und dadurch haben sich Radarsensoren in vielen modernen Fahrzeugen als Standard etabliert. Fahrerassistenzsysteme, die eine korrekte und zuverlässige Ausführung bei komplexen Fahrszenarios ermöglichen, stellen Regelungstechniker vor eine Herausforderung. Für die Entwicklung von solchen System sind Simulationen unumgänglich. Solche Simulationen benötigen in weiterer Folge realistische Sensormodelle um die Eingangsinformation zu generieren die für die zu entwickelnden Algorithmen benötigt werden. Im Rahmen dieser Arbeit wird ein generisches Radar Modell/Simulator vorgestellt. Der Simulator kann in jeder Fahrzeugsimulation basierend auf Matlab/Simulink eingesetzt werden. Bei einem gegebenen Verkehrsszenario das als Eingangsinformation dient, erfasst das Modell den Detektionsbereich des Sensors mit Hilfe eines Ray Tracing Algorithmus. Systemeigenschaften wie Antennendiagramm und Sendeleistung werden in die vom Ray Tracer erfasste Szene mit einbezogen und damit das Radarsignal generiert. Grundlegende Radar Signalverarbeitungsmethoden extrahieren Objektinformationen, die für weiterführende Simulationen verwendet werden. Der entwickelte Radar Simulator kann in echtzeitfähigen Fahrsimulatoren zur Entwicklung von Fahrerassistenzsystemen verwendet werden, aber auch für die Verbesserung von Radar Signalverarbeitungstechniken.

Symbols

Coordinate systems

x	Longitudinal direction (x-axis sensor based)	m
y	Lateral direction (y-axis sensor based)	m

Physical constant

k	Boltzmann constant	$\frac{\mathrm{J}}{\mathrm{K}}$
c	Speed of Light	$\frac{\mathrm{m}}{\mathrm{s}}$

Variables

$\mathbf{E}$	Electric field	$\frac{\mathrm{V}}{\mathrm{m}}$
$\mathbf{H}$	Magnetic field	$\frac{\mathrm{A}}{\mathrm{m}}$
$\mathbf{S}$	Poynting vector	$\frac{\mathrm{P}}{\mathrm{m}^2}$
D_E	Emitted peak power density	$\frac{\mathrm{W}}{\mathrm{m}^2}$
P_E	Peak of emitted power	W
R	Range	m^2
G	Antenna gain	
A_e	Effective aperture	m^2
ρ	Aperture efficiency	

D	Diameter	m
P_O	Power on the object	W
D_R	Power density back at sensor	$\frac{\mathrm{W}}{\mathrm{m}^2}$
P_R	Receiving power	W
σ	Radar cross section	
R_{max}	Maximum range	m
$P_{R_{min}}$	Minimum receiving power	W
N_i	Receiver noise	W
B_N	Noise bandwidth	Hz
G_{RX}	Receiver gain	
G_{norm}	Normalized gain	
P_o	Signal power output	W
P_i	Signal power input	W
F	Noise figure	
Θ	Beam width	$^\circ$
SNR_i	Signal to noise ratio input	
SNR_o	Signal to noise ratio output	
$P(\phi)$	Power density	$\frac{\mathrm{W}}{\mathrm{m}^2}$
$C(\phi)$	Directivity characteristic	
$u_t(t)$	Transmitting signal	V
r	Range	m

λ	Wavelength	m
ϕ	Phase shift	
$u_r(t)$	Received signal	V
f_D	Doppler frequency	Hz
f_r	Received frequency	Hz
f_e	Emitted frequency	Hz
$u_{t,r}$	In-phase part	V
$u_{\overline{t,r}}$	In-phase part damped	V
f_0	Carrier frequency	Hz
t_p	Pulse duration	s
Δf	Bandwidth	Hz
ϕ_D	Doppler phase shift	
t_{RT}	Time of flight	s
t_R	Time duration between transmitting signal and echo	s
f_{prf}	Pulse repetition frequency	Hz
t_{prf}	Pulse repetition time	s
$\Delta f_{\text{Dopppler}}$	Doppler frequency resolution	Hz
$\Delta\dot{r}$	Relative velocity resolution	$\frac{\text{m}}{\text{s}}$
ω_0	Carrier circular frequency	Hz
ω_i	Circular frequency	Hz
Φ_A	Beam width	$^\circ$

φ	Target angle	$^\circ$
ϵ	Failure ratio	
$P_1 - P_4$	Object coordinates	m
$\mathbf{A} - \mathbf{D}$	Intersection point matrices	
x_{Target}	Intersection point x-coordinate	m
y_{Target}	Intersection point y-coordinate	m
Δx_{edge}	Differnce last and first target point	m
Δy_{edge}	Differnce last and first target point	m
l_{edge}	Object length	m
C_{M_x}	Center of mass x-direction	m
C_{M_y}	Center of mass y-direction	m
C_M	Center of mass	m
φ_{C_M}	Center of mass angle	$^\circ$

1 Introduction

Radar sensors are used in many modern car nowadays. Improving road safety is one of the main concerns in the automotive industry. Trends in automotive development are pushing radar system technology to higher level of demand in automotive applications. The application range reaches from collision prevention assistance for advanced driving assistance systems subsequently autonomous driving to simple parking sensors [1].

Radar sensors measure information, such as range, azimuth angle and velocity of objects that are in front and within the field of view of the sensor to determine the driving situation as shown in figure 1.1. This measurements are used to provide the driving assistance systems with useful information to warn the driver or to take over control of the vehicle to avoid dangerous situations. Environmental conditions such as bad weather or no light should not limit the safety functionality of such systems.

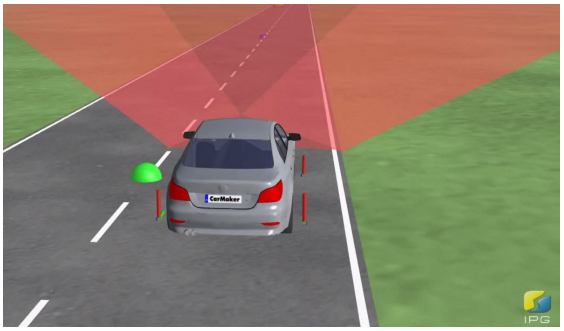

Figure 1.1: Driving scenario [2].

1.1 Radar Technology used in Automotive Applications

Radar systems in automotive applications represent detected objects like for example vehicles or pedestrians as object points. These points are described with X- and Y-coordinates and the corresponding relative velocity [3]. Dimensions like width and length are not always available, due to the alignment of the object. Radar sensors are used in automotive applications, because of there ability to provide reliable measurements at all environment conditions compared to lidar or camera based sensors. The emitted power of automotive radar sensors is usually below (10 mW), which is a harmless health

hazard for humans. Radar sensors used in automotive can be grouped into two sensor types, LRR and SRR. The LRR-sensor (Long Range Radar) is typically operating at a frequency range of (76-77 Ghz) and can have a range up to 250 meters. For a smaller range, the SRR-sensor (Short Range Radar) type is used. This sensor operates at (24-24.25 Ghz) up to a range of 80 meters [4].

LRR-Sensors can be used in following driving functions:

- ACC-adaptive cruise control
- CAS-collision avoidance system
- Autonomous driving

SRR-Sensor are used for following functions:

- PAS-parking assist system
- BSD-blind spot detection
- TJA-Traffic jam assist

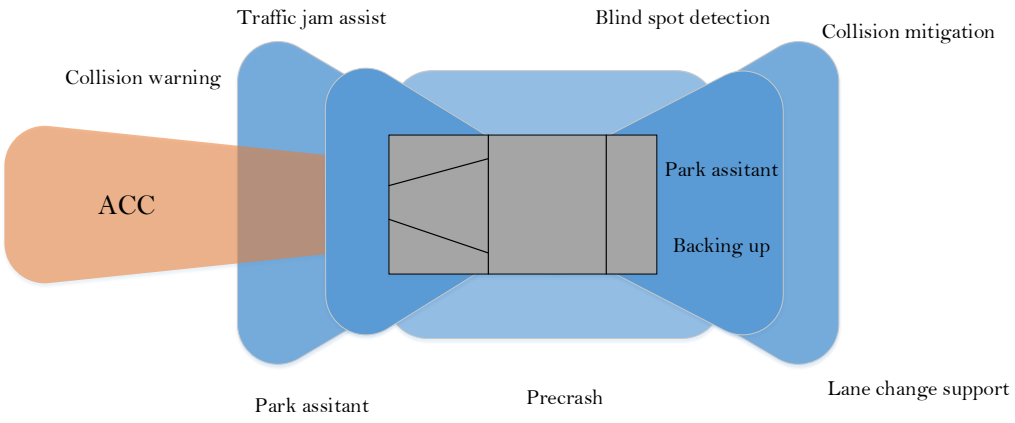

Figure 1.2: Driving assistance systems [4].

1.2 Radar Simulation

As already explained, radar sensors are used in advanced driving assistance systems. To make sure, that such systems work properly it is essential to test them [5]. Validating advanced driving assistance systems in real traffic conditions is time consuming and can lead to high costs and can be sometimes safety critical. To speed up the development of

advanced driver systems, virtual driving simulation tools are used. The validation process can be optimized by using appropriate simulations tools more frequently. Driving simulators range from expensive installations at research institutes as exemplary shown in figure 1.3 to commercially available software for personal computers as shown in figure 1.1. Driving simulators offer a promising virtual prototyping platform to test and verify advanced assistance systems in different development phases and those driving simulators need a simulation model of the radar system [7]. The behaviour of the radar must

Figure 1.3: Driving simulator NADS-1 [6].

be well understood under all road conditions, including scenarios, which are difficult to accomplish on the road or to set up on a test track. A radar sensor model should be able to handle complex traffic scenarios and to distinguish between several vehicles in the field of view of the radar sensor shown in figure 1.4.

Driving simulators, which are controlled by humans (man in the loop testing) shown in figure 1.3 need to be real time capable and therefore it is required to have a simple, relatively fast, radar simulator for advanced driver assistance systems to meet the requirements. The traffic scenarios, which are needed to ensure a reliable function of these assistance systems are captured by sensors. In the development of driver assistance systems, it is important to give those systems realistic sensor signals to ensure a correct testing of the algorithm to be implemented. Emulating real sensor signals can be challenging, due to complex traffic scenarios. Radar models can remedy this situations. There are various model approaches that range from high precision like boundary element method simulation to simple highly abstracted, idealized models to guarantee real time simulation [8].

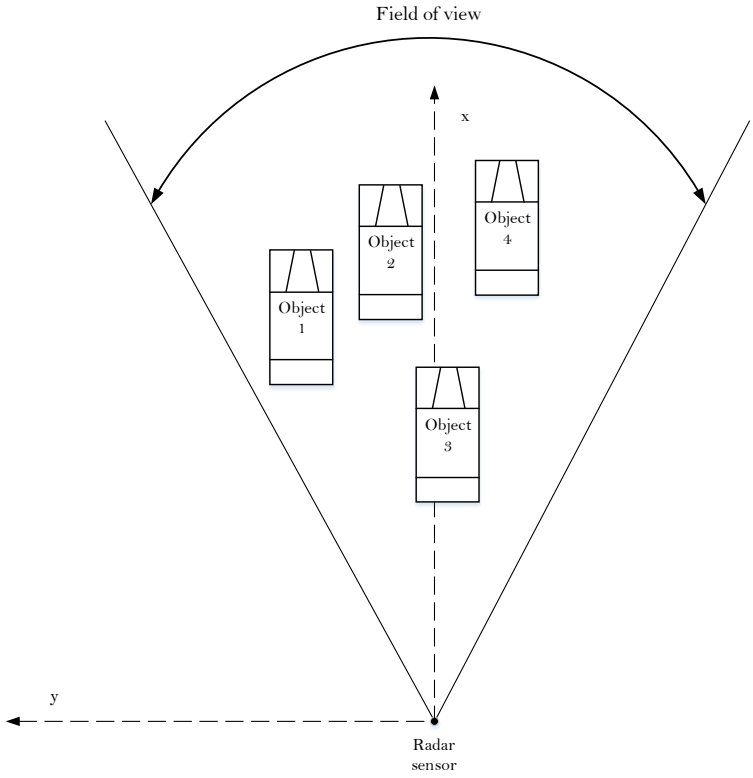

Figure 1.4: Traffic scenario in front of the radar sensor.

Some driving simulations are using a sensor model that is a simple geometrical approach. This model calculates the closest point of an object to the sensor. This is a fast and simple approach, but only the closest point to the sensor is not reliable for validation of driving assistance systems since the object can be wider or longer than a normal passenger vehicle [2].
An integration of a phenomenological radar sensor model for adaptive cruise control and auto emergency braking systems was presented here [9]. Another approach is to inject errors into the simulation that are comparable to the characteristics of real sensors. The model can modify this characteristic by setting parameters for the injected errors to adjust the behaviour of the sensor to the specific needs [10].

1.3 Thesis Outline

The use of a virtual driving environment for testing assistance systems gains more and more importance. The algorithms to be tested need to be provided with information of the vehicle environment, like distance, velocity and azimuth angle of the detected vehicle. Therefore, a generic radar sensor model is developed in this master's thesis, which considers the geometrical pattern and radar systems specifics. The traffic scenario input information of the radar sensor model is provided by the virtual driving simulation environment and the output of the model is used for further simulation steps as shown in figure 1.5. This model is suitable for object detection in real time and can be parametrized. Following this, the model is separated into four sub modules. The first

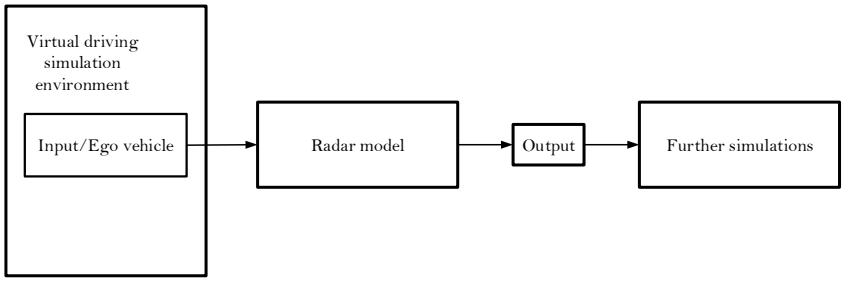

Figure 1.5: Virtual driving simulation environment.

module is a geometrical model, which scans the object within the detection range of the sensor. This information is used and merged with the characteristic of an antenna in the second part by using a convolution algorithm. The combination of the geometric model with the antenna beam yields to an radar signal that depends on the position of the object, which leads to the received power of the object by using the radar equation. The received signal is used in the third part. This module estimates the number of objects in the field of view of the sensor. The last part is the object data, which summarizes the data points and estimates the reference point.

This thesis is structured as follows. Chapter 2 describes the radar physics used in the radar simulation. Chapter 3 introduces different radar systems and explains the measurement of angular positions. Chapter 4 then includes the result from the previous chapters into the modelling process and presents the proposed sensor model.

2 Radar Physics

The word radar is an abbreviation for RAdio Detection And Ranging. A Radar is an electromagnetic system that is used for detection and location of objects. It operates by transmitting a particular type of waveform and detects the receiving echo signal. Many radar systems are using modulated waveforms and directive antennas to transmit electromagnetic energy into a specific volume in space to search for objects. Objects, which are in the search area of the radar will reflect some portions of the power back to the radar.

This receiving power is then processed by the radar receiver to extract information such as range, velocity, angular position and other target identifying characteristics. The distance or range is a very important attribute. Other systems, such as infrared or video sensors can also be used to estimate the same object information such as range and velocity. But, radar sensors have a significant advantage of being resistant against bad environmental and weather conditions. This chapter will discuss the radar physics and radar systems used in automotive applications. The radar physics and basics will help to understand the sensor simulation process. Literature that cover this topic can be found in [11],[12] and [13].

2.1 Electromagnetic Wave Propagation Basics

An electromagnetic wave is a transversal wave and can be generated by using a dipole, which can be explained as a resonant circuit [14]. The basic concept is shown in 2.1. Every resonant circuit has an inductor L and a capacitor C. The energy moves from the inductor to the capacitance and back again. This creates an electric field $\mathbf{E}$ in the capacitor between its plates and a magnetic field $\mathbf{H}$ in the inductor. The electric field and magnetic field are changing periodically. The electric field is between the capacitor plates and has no impact in open air, due to the small capacitor plate spacing. By increasing the spacing between the capacitor plates the electromagnetic field can propagate to the outside shown in figure 2.2. Figure 2.3 shows the open LC resonant circuit. With an signal source applied at the center of the open LC circuit, the oscillating current through the antenna will create a magnetic field and the charge of the electrons produces an electric field. These two fields will radiate away from the antenna into space as an electromagnetic wave. The electromagnetic wave as explained, consists of two fluctuating fields, one is the electric $\mathbf{E}$ and the other magnetic $\mathbf{H}$ shown in figure 2.4. The two fields are in phase and perpendicular to each other, and both are perpendicular

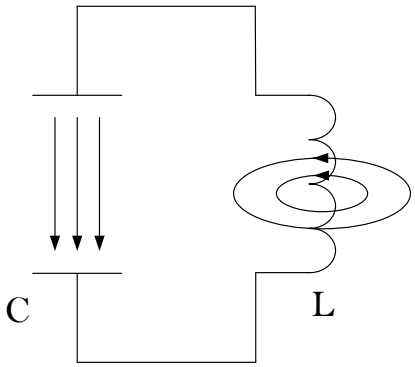

Figure 2.1: LC circuit.

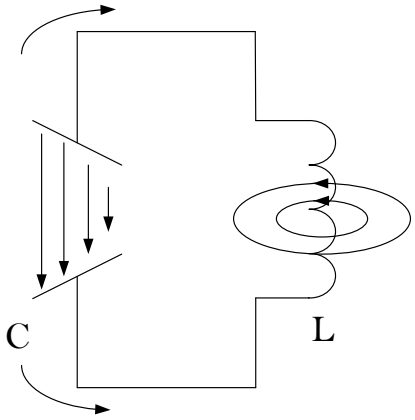

Figure 2.2: Increasing capacitor plate spacing.

to the direction of the power transfer. These fields propagate in free space at the speed of light. The quantity that describes the power density is called Poynting vector [15]

$$\boldsymbol{S} = \frac{\mathbf{1}}{\mathbf{2}}\boldsymbol{E} \times \boldsymbol{H}^{*}. \tag{2.1}$$

The Poynting vector describes the power density of of an electromagnetic field.

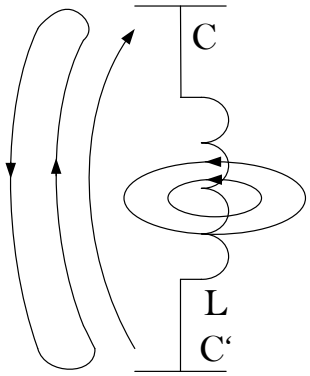

Figure 2.3: Open LC circuit.

2.2 Simple Radar

The principle of wave propagation was explained above. The basic principle of a radar is that it transmits pulses of electro magnetic waves, which are reflected from objects in their direction. The object reflects the wave back to the sensor. A block diagram for a radar system is shown in figure 2.5, which gives a good overview of the radar sensor. The transmitter generates a pulse of electromagnetic energy, which is oscillating at a certain frequency and duration. The pulse is routed through a transmit receive switch to an antenna. The switch protects the sensible receiver from the high power transmitted pulse. The antenna is responsible for the radiation of the signal into free space. Travelling at speed of light, the electro magnetic wave propagates through the medium and reflects from the objects it impinges.

The reflected signal that turns back to the radar, is received by the antenna and routed by the switch to the receiver. The received signal can be detected by the receiver, because it imitates the emitting signal in frequency and duration. Interfering signals are filtered and measurements of the obstacles are made by signal processing. A time measurement is made when the signal is emitted and when the signal is received. Following this, the range can be easily determined by

$$R = \frac{c\Delta t}{2}. \tag{2.2}$$

The distance covered by the electro magnetic wave is twice the range, because the wave radiates to the object and back to the radar [13].

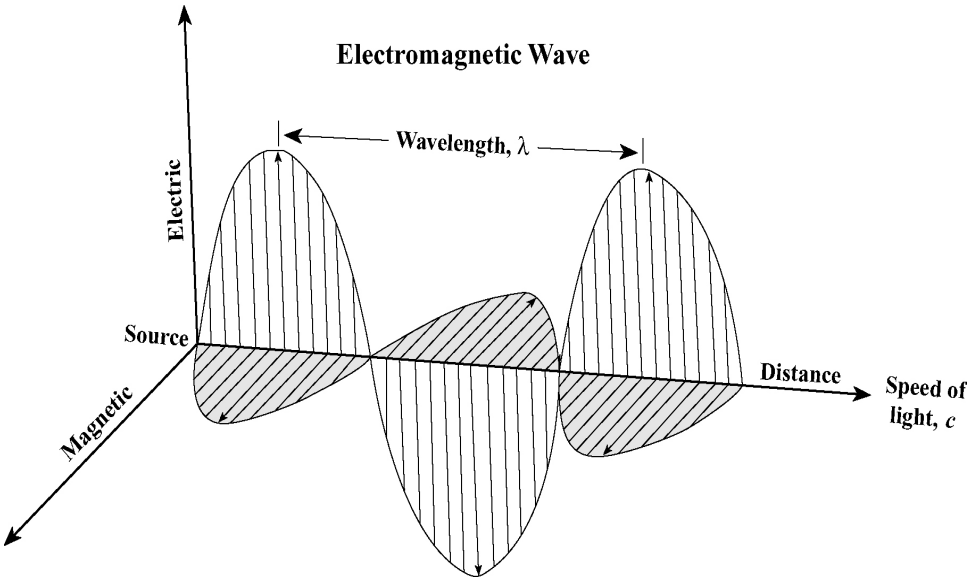

Figure 2.4: Electromagnetic wave [16].

2.3 Radar Equation

One important part in radar theory is the radar equation, which is valid for total incoherent scattering. This means that no rays can interfere with each other. If the ray would be coherent the emitting and receiving ray could interfere with each other. Additional to this, the following assumptions have to be made:

- The electromagnetic waves propagates unimpeded between radar and target
- Homogeneous propagation medium

Literature can be found in [11],[12].

2.3.1 Derivation of the Radar Equation

The radar equation represents the physical dependences of the transmitting power up to the receiving of the echo-signals. The receiving power P_R at the sensor input is given by the radar equation, depending on the transmitted power P_E, the distance R and the reflecting characteristics (described as radar cross section σ) of the object. At known sensitivity of the radar receiver, the radar equation determines the theoretically maximum range. Consider a radar with an isotropic source of an electromagnetic pulse of peak power P_E radiating into free space. An isotropic radiator is a point source of electromagnetic wave, which radiates in all directions with the same intensity. It has

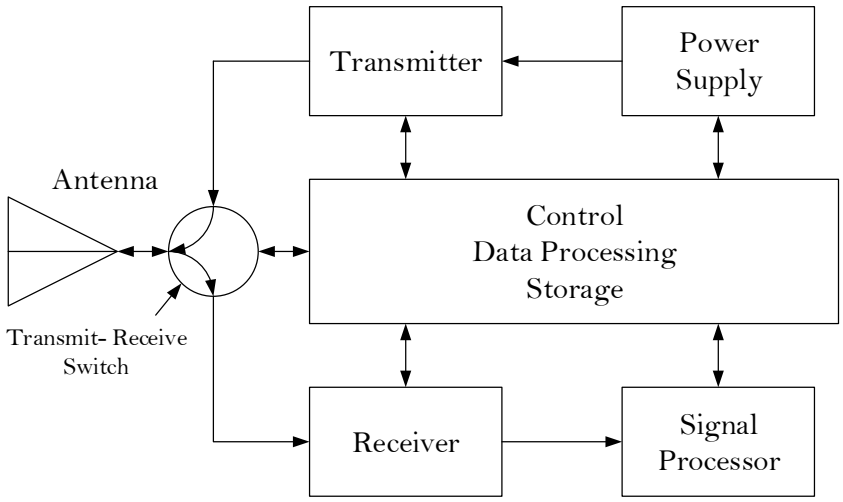

Figure 2.5: Radar block diagram.

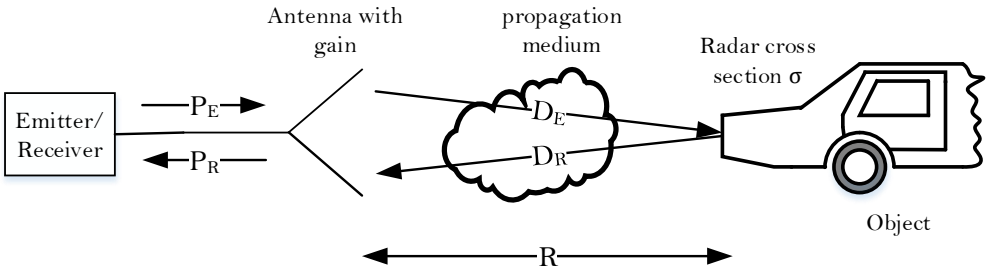

Figure 2.6: Schematic for the radar equation.

no preferred direction of radiation. Due to this characteristic, the peak power density (power per unit area) at any point in space on a sphere is

$$D_E = \frac{\text{Peak of emitted power}}{\text{area of a sphere}} \quad \text{in} \quad \frac{\text{watts}}{\text{m}^2}. \tag{2.3}$$

Assuming a lossless propagation medium, the power density at distance R is

$$D_E = \frac{P_E}{4\pi R^2}, \tag{2.4}$$

where P_E is the emitted peak power and $4\pi R^2$ the surface of a sphere of radius R. To increase the power density in one certain direction radar system utilize directional antennas. This is expressed by the antenna gain. A directive antenna is usually characterized

by the antenna gain G and effective aperture A_e. This is described in the following equation

$$G = \frac{4\pi A_e}{\lambda^2} \tag{2.5}$$

where λ is the wavelength. The link between the effective aperture A_e and the physical aperture A is the aperture efficiency ρ. The effective antenna aperture A_e is defined as

$$A_e = \rho A, \tag{2.6}$$

with

$$0 \leq \rho \leq 1, \tag{2.7}$$

is a measure of the area of the receiving antenna that intercepts the receiving signal. Good antennas have a aperture efficiency ρ close to one. For further steps A_e and A will be the same. This means that the receiving and emitting parts of the antenna will have the same gain G. The antenna gain also depends on the azimuth and elevation beam width of the antenna by

$$G = k\frac{4\pi}{\theta_e \theta_a} \tag{2.8}$$

where $k \leq 1$ and depends on the physical aperture shape. The azimuth and elevation beam width of the antenna are θ_a and θ_e. Figure 2.7 shows the effective aperture in circular shape with the diameter D. This gives an actual area A of

$$A = \frac{\pi D^2}{4} \tag{2.9}$$

and an effective area A_e of

$$A_e = \frac{\rho \pi D^2}{4}. \tag{2.10}$$

As D increases, gain and effective aperture both increase. For a directive gain G, the directional isotropic power density D_E for an object at a distance R is

$$D_E = \frac{P_E G}{4\pi R^2}. \tag{2.11}$$

When the emitting power impinges on an object, parts of the power will be backscattered. The amount of the reflected power is proportional to the target size, orientation, physical shape and material, which is summarized in one parameter called the radar cross section (RCS) denoted by σ. The power incident on the object is

$$P_O = \frac{P_E G \sigma}{4\pi R^2}. \tag{2.12}$$

The object acts as a source of radiation $P_O = \frac{P_E G \sigma}{4\pi R^2}$ having an isotropic scattering pattern at a certain distance. Now, the power density back at the sensor, at distance R, is given by

$$D_R = \frac{P_E G \sigma}{4\pi R^2 4\pi R^2} = \frac{P_E G \sigma}{(4\pi)^2 R^4}. \tag{2.13}$$

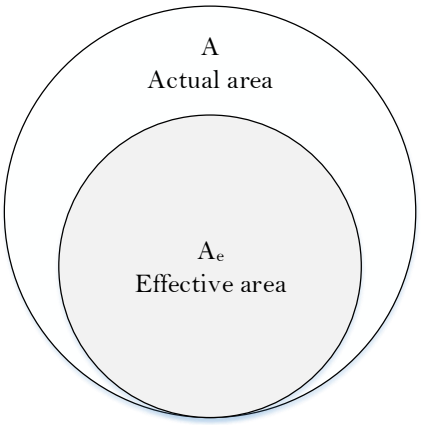

Figure 2.7: Effective aperture circular shape.

At the radar sensor the receiving power P_R

$$P_R = \frac{P_E G \sigma A_e}{(4\pi)^2 R^4}, \tag{2.14}$$

depends on the power density D_R at the sensor site and the effective antenna aperture A_e. The formula above can be rewritten to

$$R^4 = \frac{P_E G \sigma A_e}{(4\pi)^2 P_R}, \tag{2.15}$$

in order to calculate the range R. Equation (2.15) represents the basic radar equation. The maximum distance R_{max} can be determined by using the minimum detectable receiving signal power $P_{R_{min}}$. Equation (2.15) can now be rewritten to

$$R_{max} = \sqrt[4]{\frac{P_E \sigma A_e^2}{(4\pi)^2 P_{R_{min}}}}. \tag{2.16}$$

In order to double the distance maximum of the radar, equation (2.16) suggests that the peak emitted power P_E must be increased sixteen times or increase the effective antenna aperture A_e four times. The radar distance is relatively insensitive to the emitted power, due to the fourth of root law in the radar equation [17].

2.3.2 Losses

Equation (2.16) gives a theoretical number for the maximum detection range, but there are other losses that have to be considered. Such losses include atmospheric and system

losses (ohmic losses). The atmospheric losses are causing an attenuation and scattering to the electromagnetic signal. These losses increase at higher frequency or at adverse environmental conditions (rain, fog) [18],[12].

Temperature and atmospheric pressure can also vary the signal. So the atmospheric loss factor is denoted by L_A. Losses that have to be considered are:

- Transmitter losses : Occur between radar transmitter and antenna input port (transmission line) and are called plumbing losses.
- Receive losses : Occur between radar receiver and antenna input port.
- Antenna pattern loss and scan loss : Occur when the antenna gain is not fully aligned to the object.

The antenna mismatch losses have been already accounted in the antenna gain term. The total system losses are denoted with the factor L_{sys}. By including this losses the radar equation is

$$R_{max} = \sqrt[4]{\frac{P_E \sigma A_e^2}{(4\pi)^2 P_{R_{min}} L_A L_{sys}}}. \tag{2.17}$$

2.3.3 Receiver Noise

In practical situations the receiving signal will be corrupted with noise. This can lead to wrong detection. Noise is generated by atmospheric and manufactured sources (other auto mobiles, power facilities, other radars) explained in section 2.3.2 and can be described by its PSD function (Power Spectral Density) [11]. However, the most noise that is generated is in the frontend of the receiver, particularly by the first amplifier and mixer stages [13].

The generated noise in the frontend of the receiver is known as thermal noise. Thermal noise is generated in conductors and semiconductors and sets the limit on the receiver sensitivity [12]. Thermal noise is effectively white noise and extends over a very wide spectrum. It arises due to random thermal fluctuations of electrons in conductors and this results in a random current flow and therefore random noise voltages across resistances. The thermal noise voltage has a Gaussian PDF (Probability Density Function). Thermal noise power N_i is given by

$$N_i = kTB_N, \tag{2.18}$$

where k is the Boltzmann's constant (1.38×10^{-23} J/K), T is the temperature in degrees Kelvin (K) and B_N is the noise bandwidth in Hz. A standard Temperature of 290 K is taken as a reference. This leads to a noise power density of

$$N_i = 4 \times 10^{-21} \ \frac{\mathrm{W}}{\mathrm{Hz}}.$$

2.3.4 Noise Figure

The components of the receiver are also adding additional noise onto the signal path and reduce the signal to noise ratio of the object signal. The performance of the receiver is described by the noise figure F.

The noise figure is the ratio between the input SNR_i and the output SNR_o as shown in equation (2.24). The noise figure F can be interpreted as the factor by which the noise on the output of an ideal device must be increased to give the same noise level out of the actual device with the same overall gain and bandwidth. Schematic 2.8 illustrates the noise figure. As seen in figure 2.8 there is an signal power P_i and a noise power N_i on the input of the receiver, which results with the receivers noise to the signal power P_o and a noise power N_o at the output. Under ideal conditions, N_i is thermal noise only,

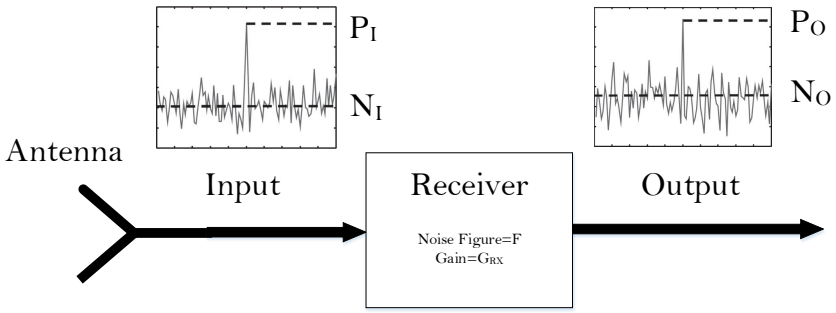

Figure 2.8: Illustration of the noise figure.

which is (2.18). The gain of the receiver is

$$G_{RX} = \frac{P_o}{P_i}. \tag{2.19}$$

Therefore, the signal power at the output is

$$P_o = G_{RX} P_i. \tag{2.20}$$

For an ideal receiver the noise power output would be

$$N_o = G_{RX} N_i. \tag{2.21}$$

With the definition of the noise figure, the actual noise at the output is

$$N_o = F G_{RX} N_i. \tag{2.22}$$

Substituting equation (2.18),(2.19) into (2.22) gives

$$N_o = k T_0 B_N F (P_o/P_i). \tag{2.23}$$

Rewriting (2.23) for F gives

$$F = \frac{\mathrm{SNR}_i}{\mathrm{SNR}_o}, \tag{2.24}$$

where SNR_i

$$\mathrm{SNR}_i = \frac{P_i}{N_i} \tag{2.25}$$

and SNR_o

$$\mathrm{SNR}_o = \frac{P_o}{N_o} \tag{2.26}$$

are the corresponding SNRs for the input and output. According to [12], This relationship is only valid for the circumstance that N_i is thermal noise only. Equation (2.24) does not hold when external noise is received by the radar sensor. However, equation (2.24) is a useful illustration of the fact that the noise figure of a receiver degrades the signal to noise ratio. An ideal receiver would have a noise figure value of $F = 1$ (0 dB) and this will lead to equal input and output signal to noise ratios. A practical receiver [12] would have a noise figure value of $F < 1$ ($F > 0$ dB) and this would result in a lower output SNR compared to its input SNR.

2.3.5 Minimum Detectable Signal Power

Equation (2.16) gives

$$P_i = kT_0B_NF(P_o/N_o), \tag{2.27}$$

or rewritten with SNR_o

$$P_i = kT_0B_NF(\mathrm{SNR}_o). \tag{2.28}$$

The minimum detectable signal power can be written as

$$P_{min} = kT_0B_NF(\mathrm{SNR}_o)_{min}. \tag{2.29}$$

The minimum input signal power is estimated by using the minimum signal to noise ratio of the output to meet the desired detection performance. Now, the radar equation can be put in the final form, by using equation (2.29) in (2.17) the result is

$$R_{max} = \sqrt[4]{\frac{P_E\sigma A_e^2}{(4\pi)^2kT_0B_NF(\mathrm{SNR}_o)_{min}L_AL_{sys}}}. \tag{2.30}$$

2.4 Antenna

An antenna is a device which converts electric power into electromagnetic waves and vice versa. The antenna transmits and receives electromagnetic waves. Especially for radars, it is important that the antenna enhances the performance. In emitting mode a signal source supplies the antenna terminals and the antenna radiates the power from

the signal source as an electromagnetic wave into space. The receiving mode produces voltage at the antenna terminals due to the incident electro magnetic wave. Typically an antenna consists of an arrangement of metallic conductors that are connected to the receiver or transmitter. Literature covering this section are [14], [19].

2.4.1 Antenna Characteristics

Antennas are characterized by a number of parameters. The most important are:

- Antenna pattern
- Antenna gain
- Beam width
- Major and side lobes (minor lobes)
- Front to back ratio
- Aperture

2.4.1.1 Antenna Pattern

Radar sensors in automotive applications are using directional antennas. Additional information that covers this section can be found in [14], [20]. A directional antenna is referred to as anisotropic antenna. The power, which is radiated by the antenna forms a field that has a defined radiation pattern (or antenna pattern). A radiation pattern defines the variation of the power radiated by an antenna as a function of the direction away from the antenna. To plot an antenna pattern, two different types of graphs are used, which are the rectangular and the polar graph.

The polar coordinated graph proved to be useful in the studying and comparisons of radiation patterns. An exemplary antenna pattern is illustrated in figure 2.9. The same antenna pattern in rectangular graph is shown in figure 2.10. The horizontal axis in this pattern corresponds to the circular axis of the polar coordinate graph and the vertical axis to the radius of the polar coordinate graph. Both graphs are in logarithmic scale, but they can also be scaled linear. For studying radiation patterns the logarithmic scale is more suitable then the linear scaled pattern.

The area around the direction of maximum radiation is called main lobe or main beam. The region is usually defined by the -3 dB of the main beam. Directive antennas have the ability to direct waves into one specified direction, the lobe in this direction is bigger than the other lobes shown in figure 2.9 and 2.10. The radiation of the antenna interferes at some angles with other parts of the antenna and cancels the antenna radiation almost completely out. This behaviour is called null radiation shown in figure 2.10.

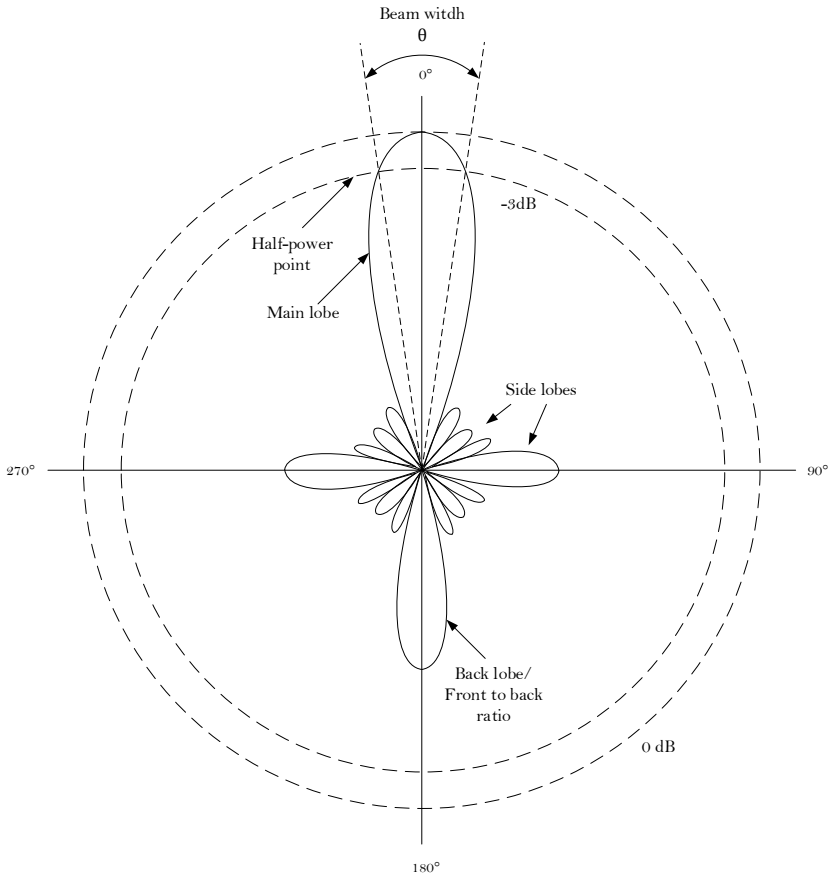

Figure 2.9: Antenna pattern in a polar coordinate graph.

2.4.1.2 Antenna Gain

Isotropic antennas or spheric antennas radiate the signal power in every direction equally, where as anisotropic antennas or directional antennas radiate in one direction more than in another. This means more power is emitted in one certain direction. The ratio between the amount of energy that would radiate in this certain direction compared to an antenna with isotropic radiation is defined as the antenna gain. In previous section 2.3 the radar equation was derived under the assumption, that the radar antenna is perfect aligned on the radar target. The antenna gain will be lower, for objects that are not aligned perfectly to the main beam of the antenna [19]. Figure 2.11 shows the directivity pattern $G(\theta)$ in azimuth angle. The distribution of the emitting power as a function of ϕ is given by the power density $D(\phi)$ (W/m^2). By integrating the power

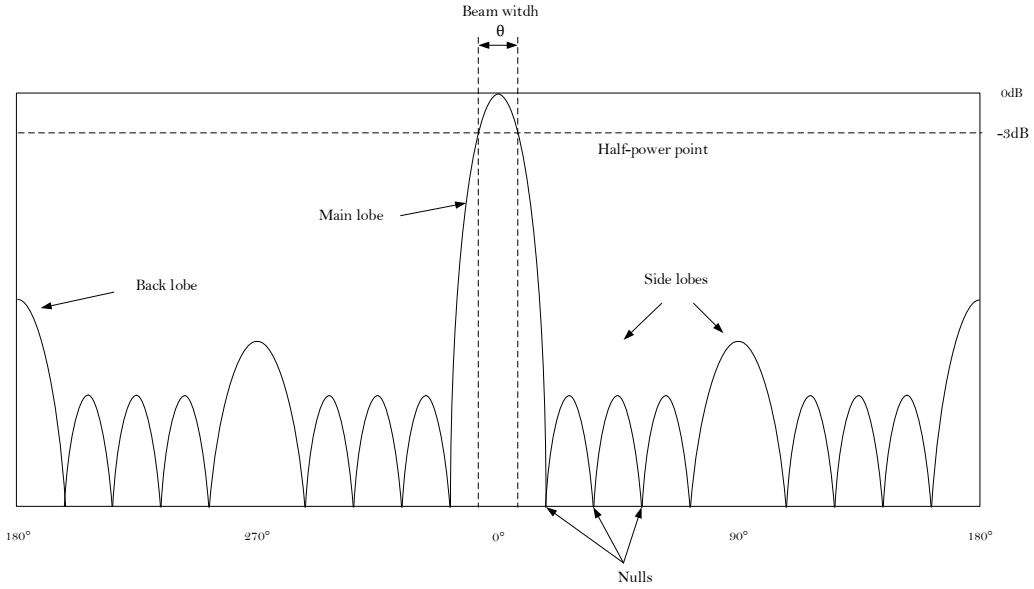

Figure 2.10: Antenna pattern in a rectangular coordinate graph.

density $D(\phi)$ over the azimuth angle ϕ, the emitting power is

$$P_E = \int_{\phi_1}^{\phi_2} D(\phi) d\phi. \tag{2.31}$$

The directivity characteristic $C_D(\phi)$

$$C_D(\phi) = \left| \frac{D(\phi)}{D_{max}} \right|, \tag{2.32}$$

can be determined by using $D(\phi)$ and D_{max} ($\phi = 0$). The directivity characteristic $C_D(\phi)$ and maximum Gain G_{max} results in an angle dependent gain

$$G(\phi) = G_{max} C_D(\phi). \tag{2.33}$$

2.4.1.3 Beam Width

The beam width is the angular range of the antenna in which half of the signal power is still emitted. The bordering lines at which the signal power falls to 50% respectively -3 dB is shown in figure 2.9, 2.10 and 2.11. This angle is then described as beam width or half power angle/point (-3 dB) and is notated as θ.

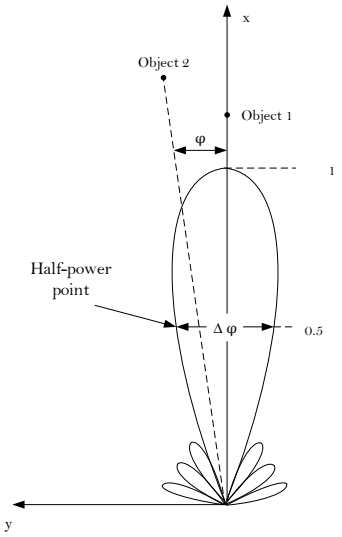

Figure 2.11: Normalized directivity pattern.

2.4.1.4 Main Lobe and Side Lobes (Minor Lobes)

As explained in previous sections of the antenna characteristics, the main lobe has the largest gain. The other lobes are called side lobes and are representing unwanted radiation and this radiation should be minimized. The lobe that is in the opposite direction than the main lobe is called back lobe. The ratio between the main lobe and the back lobe is called front to back ratio. A high front to back ratio is desirable, because this means that a minimum signal energy is emitted in the unwanted direction.

2.4.1.5 Aperture

The effective aperture or effective area A_e of a receiving antenna is defined as the area, oriented perpendicular to the direction of an incoming radio wave, which describes the amount of captured power from a given radar wave. For example, if the receiving power density of the wave is 1 mW/m^2 and the effective Aperture A_e is 10 m^2, the receiving signal power results in 10 mW. Figure 2.7 shows the difference between effective antenna area A_e and antenna area A. In the radar equation section 2.3, the aperture was already explained in detail.

2.5 Radar Cross Section (RCS)

2.5.1 Definition

The RCS of an object is its equivalent reflected area and has the unit (m^2). Literature provided in [12], [11] and [13] covers this section. Electromagnetic waves, with any specified polarization, are scattered in all directions when they impinge on an object. Those electromagnetic waves are separated up into two parts. The first part of the wave has the same polarization as the receiving antenna. The other part of the wave has a different polarization as the receiving antenna and this is why the antenna will not respond to the signal. The wave, which has the same polarization as the antenna is used to defined the object RCS. When a object is illuminated by the emitting energy of the sensor, it will act like an antenna and will have near and far fields. Waves reflected and measured in the near field are, in general, spherical. In the far field the radar waves are a linear combination of plane waves. Assume the power density of an emitting wave at distance R is D_E.

The obtained reflected power from the object is

$$P_O = \sigma D_E, \tag{2.34}$$

where σ is the radar cross section of the object. D_R is defined as the power density

$$D_R = \frac{P_O}{4\pi R^2}, \tag{2.35}$$

of the reflected wave at the receiving antenna. Using equation (2.34) and (2.35) results in

$$\sigma = 4\pi R^2 \left(\frac{D_R}{D_E}\right). \tag{2.36}$$

To ensure that the receiving antenna is in the far field (i.e. scattered waves received by the antenna are planar) equation (2.36) needs to be completed with the limes to infinity

$$\sigma = 4\pi R^2 \lim_{R\to\infty} \left(\frac{D_R}{D_E}\right). \tag{2.37}$$

This definition assumes isotropic scattering from a perfectly reflective body. The radar cross section in equation (2.37) is defined as the target radar cross section (RCS).

2.5.2 Factors Determining Radar Cross Section

Many objects that are impinged by an electromagnetic wave have a complex geometry and they consists of a wide variety of materials. These objects/targets have a complicated array of scattering centers that reflect, diffract and refract the signal back to the receiving radar. Some reflection may be associated with structural circumstances of the object,

or some arise between multiple features (Range, Antenna polarization). The return of these waves is combined into a sum of all these different features. The radar cross section depends on following parameters:

- Object geometry (size, shape, orientation)
- Object composition
- Angle of illumination/reception
- Transmitted popularization
- Receiver polarization
- Range
- Frequency

At very short distances also the range may become a factor, because waves in the near field are in general, spherical and in the far field it is assumed to be a plane wave that is illuminating the object. Equation (2.37) indicates that RCS is defined as a far field limit, since it is based on the limit that the range becomes infinitely. For some reasons the frequency can become a significant characteristic. When the wavelength is considerably bigger then the dimension of the object, its cross section will reduce with increasing frequency. This phenomena is called Rayleigh scattering in which

$$\sigma \propto f^4, \tag{2.38}$$

holds. When the wavelength is considerably less then object dimensions, the radar cross section becomes constant. This is known as the optical region. Following this, the behaviour of the electromagnetic wave can be modelled as a ray. In case that the wavelength is similar to the object dimension, interference will occur and the RCS will fluctuate rapidly with frequency. This is known as the resonance region. The RCS is also sensitive to the angle of illumination, because complex objects have a considerable variation over small angular increments.

Exact estimation of RCS is complex. Differential or integral equations need to be solved that describe the scattering waves under the proper set of boundary conditions. Approximate methods become the reasonable choice for solving. The approximated solutions are valid in the optical region. Most approximate methods can predict RCS within few dBs of the truth [11].

A metal plate [21], that is orientated orthogonal at long distances to the emitting waves has a RCS of

$$\sigma_{\text{plate}} = \frac{4\pi A_e^2}{\lambda^2}. \tag{2.39}$$

For a plane area of 4 m^2 and a wave frequency of 76.5 Ghz ($\lambda \approx 4$ mm) the RCS value is 12.5×10^6 m^2. However, rotating the plane area by one degree at a distance of 60 m

the reflection would completely break down [21]. Both possibilities are shown in figure 2.12(a) and 2.12(b). The only reflection that would be remaining comes from the edges and the part that repels back from the surface.

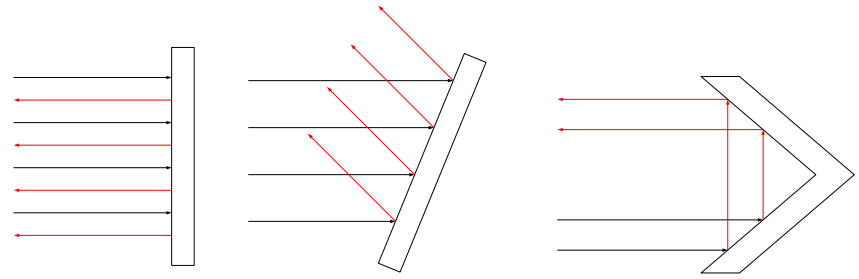

(a) 90° reflection (b) ≠ 90° reflection (c) 90° retro reflector

Figure 2.12: Reflection example.

An ideal retro reflector as shown in two dimensional in figure 2.12(c) has three mutually perpendicular reflective surfaces, placed to form the corner of a cube [21]. A perfect aligned retro reflector will reflect all signals back to the receiver, that are noticeably smaller than the object dimensions.

Vehicles with concave surfaces or plane surfaces that reflect away have a small radar cross section value. Large values cross section values can be related to retro reflectors. The u-profile that holds the crash barrier at highways has relativity high cross section value. This leads to a large number of false targets in the object list of the radar sensor. That's why it's difficult to realize an object classification only via the RCS [21],[11].

3 Radar Systems

The previous chapter was focused on the wave propagation and scattering. This chapter explains the measurement of the relative velocity and distance in different radar systems. As shown in figure 3.1 the electro magnetic wave is the carrier of the target information. Radar systems differ from each other by the type of modulation of the carrier signal at the transmitter. Another modulation of the electromagnetic wave will occur at the object, due to the Doppler effect when the object is moving. This will result in a phase difference between emitting and receiving signal. The Doppler effect is used to determine the relative velocity and will be explained in the next section. These books give a good overview about radar systems and the Doppler effect [21],[22],[23].

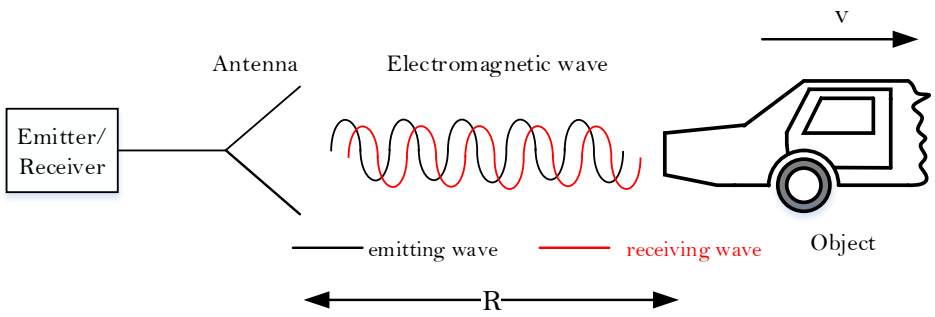

Figure 3.1: Radar-Target scenario.

3.1 The Doppler Effect

Continuous wave (CW) radar is a type of radar system, which transmits a continuous signal of constant power level and frequency [23]. The mathematical description of a continuous signal is

$$u_t(t) = A_t \cdot \cos(2\pi f_0 t + \phi_0), \tag{3.1}$$

which is used to describe the emitting signal. The echo signal is received and processed permanently. The Doppler effect causes the echo/received signal to have a different frequency. The shift of the frequency depends on the relative velocity between the target and the receiver [21]. To derive the Doppler effect, a scenario as depicted in figure

3.1 is considered. For a distance R between the antenna and the target, the wave is covering N

$$N = \frac{2r}{\lambda}. \tag{3.2}$$

wavelengths. The wave is propagating to its target and back to the receiver. Following this, the distance covered is $2r$. This corresponds to a phase shift of

$$\phi = -2\pi N. \tag{3.3}$$

If the object is moving ($v = \dot{r} \neq 0$) the phase will also change by

$$\dot{\phi} = -2\pi \dot{N} = \frac{-4\pi \dot{r}}{\lambda}. \tag{3.4}$$

With this information the receiving signal $u_r(t)$ can be rewritten by using equation (3.1) to

$$u_r(t) = A_r \cdot \cos(2\pi(f_0 - 2\dot{r}/\lambda)t + \phi_r). \tag{3.5}$$

This effect is the Doppler effect. It causes a difference frequency between receiving signal and emitting signal. The Doppler frequency f_D is defined as

$$f_D = -\frac{2\dot{r}}{\lambda} = -\frac{2\dot{r}f_0}{c}. \tag{3.6}$$

For a receding object $\dot{r} > 0$ holds, hence

$$f_D < 0 \tag{3.7}$$

the Doppler frequency shift will be negative. The receiver frequency f_r

$$f_r = f_D + f_0, \tag{3.8}$$

will be smaller than f_0. Thus

$$f_r < f_0 \tag{3.9}$$

holds. For an approaching object $\dot{r} < 0$ holds, hence

$$f_D > 0 \tag{3.10}$$

the Doppler frequency shift will be positive. Thus

$$f_0 < f_r \tag{3.11}$$

holds.

The Doppler frequency is zero for objects that have the same relative velocity as the source object. Continuous Wave radars can only measure the relative velocity, the distance can not be measured. The CW radar is transmitting an unmodulated wave. To extract the information of distance the emitting signal needs to be modulated.

3.2 Basic Principle of Modulation and Demodulation

The process of adding information to the emitting signal is called modulation and the process of retrieving information out of a signal is known as demodulation. The electromagnetic wave is the carrier signal for the information. Besides the already mentioned CW radar, any other radar system uses a modulation of the transmitted signal. The receiving signal needs to be demodulated, to extract the information. In other terms, the emitting signal needs a marked wave front for signal recognition and a time base between emitting and receiving signal for runtime measurements. According to (3.1) three variables amplitude A_t, frequency f_0 and phase ϕ_0 can be modulated. Amplitude modulation and frequency modulation, as shown in figure 3.2(a) and 3.2(b), are used in radar systems [21].

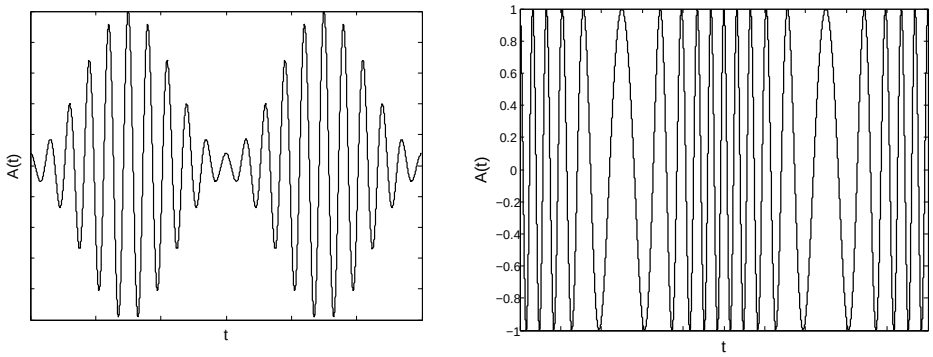

(a) Amplitude modulation example.

(b) Frequency modulation example.

Figure 3.2: Illustration of modulation examples.

3.3 Pulse Doppler Radar

Pulse modulation is a form of amplitude modulation, where the message information is encoded in the amplitude of pulses. The modulated pulses are generated by a fast switching transistor. The pulse Doppler radar determines the distance to a target by measering the time of flight between transmitted and a received pulse. Additionally the Doppler effect can be used to determine the relative velocity of the target. The radar is sending and receiving time delayed pulses. For a given pulse duration t_p, a signal with the carrier frequency f_0 is being emitted [24]. When the transmitting of the signal is finished, the radar switches to the receive mode, in order to evaluate the reflected receiving signals. The distance r results in

$$r = \frac{t_R \cdot c}{2}, \tag{3.12}$$

where c is the speed of light and t_R is the time duration between the transmitting signal and the return of the echo. The transmitting and receiving process is repeated with a pulse repetition frequency of

$$f_{\text{prf}} = \frac{1}{t_{\text{prf}}}. \tag{3.13}$$

where t_{prf} is the pulse repetition time. Figure 3.3 illustrates the timing sequence of the emitting and receiving process, where "Echo" marks the received signal. The pulse

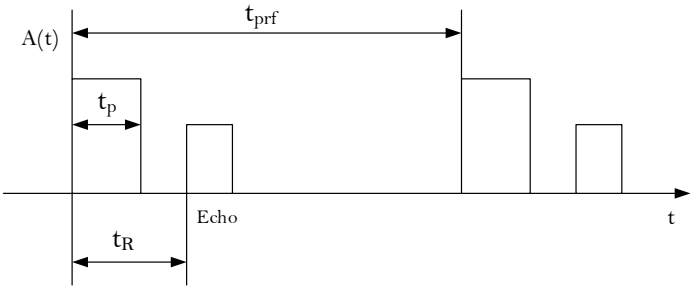

Figure 3.3: Pulse Doppler radar example.

Doppler radar can use the same antenna for the emitting and receiving mode. The detection characteristic of the pulse Doppler radar is defined by the carrier frequency f_0, pulse repetition frequency f_{prf} and the pulse duration t_p.

Given this setting, the timing allows a maximum achievable range of

$$r_{\text{max}} = \frac{ct_{\text{prf}}}{2}, \tag{3.14}$$

where t_{prf} is the pulse repetition time. For several objects, multiple echos occur. In order to separate them by means of the received echo signals, the pulse duration t_p has to be smaller than

$$\Delta r = \frac{ct_p}{2}. \tag{3.15}$$

The relative velocity is

$$v_{rel} = -\frac{\lambda f_D}{2} \tag{3.16}$$

and is achieved by the measurement of the Doppler frequency.

3.4 Frequency Modulation

Frequency modulation is a modulation method that uses a time varying frequency

$$f_0(t) = \omega_0(t)/2\pi, \tag{3.17}$$

to modulate the carrier frequency. A frequency modulated signal is shown in figure 3.2(b). A widely used frequency modulation scheme is the frequency modulated continuous wave (FMCW). The FMCW method transmits and receives the signal continuously. In contrast to the CW radar the FMCW radar changes its operating frequency during the measurement process. The distance measurement is accomplished by comparing the frequency of the received signal and the frequency of transmitted signal. A mixer produces a base band signal at the instantaneous difference frequency between the transmitting signal and the receiving signal. This will be explained in the next subsection [4]. The FMCW method will be continued in section 3.4.2.

3.4.1 Signal Mixing

A process, where at least two signals are multiplied is called signal mixing [21]. The product of two harmonic signals (3.1) with frequency f_1 and f_2 and phase shift ϕ_1 and ϕ_2 can be expressed as a sum of two harmonic waves by using the angle summation formula

$$\cos(x) \cdot \cos(y) = \frac{1}{2}\left(\cos(x-y) + \cos(x+y)\right). \tag{3.18}$$

The product of equation (3.1) and (3.5) is

$$u_{t,r}(t) = \{A_t \cdot \cos(2\pi f_0 t + \phi_0)\} \cdot \{(A_r \cdot \cos(2\pi(f_0 - 2\dot{r}/\lambda)t + \phi_r)\}, \tag{3.19}$$

and can be rewritten, by using the angle summation formula (3.18) to

$$u_{t,r}(t) = \frac{1}{2}A_t A_r \left\{\cos\left(2\pi\left(\frac{2\dot{r}}{\lambda}t\right) + \phi_0 - \phi_r\right) + \cos\left(2\pi\left(2f_0 - \frac{2\dot{r}}{\lambda}\right)t + \phi_0 + \phi_r\right)\right\}. \tag{3.20}$$

The second term of equation (3.20) has high frequency. This component is removed from the signal by the hardware of the radar (Amplifier, low pass filter). Only the low frequency part remains, which is

$$u_{\overline{t,r}} = \frac{1}{2}A_r A_t \cdot \cos\left(2\pi\left(\frac{2\dot{r}}{\lambda}\right)t + \phi_0 - \phi_r\right), \tag{3.21}$$

or

$$u_{\overline{t,r}} = \frac{1}{2}A_r A_t \cdot \cos\left(\left(\frac{\omega_0}{c}2\dot{r}\right)t + \phi_0 - \phi_r\right). \tag{3.22}$$

The information of the Doppler shift is in the argument of the cosine. The information that is processed, is now in the low frequency range.

3.4.2 Frequency Modulated Continuous Wave (FMCW) continued

The linear FMCW radar modulates the instantaneous frequency by means of a sawtooth signal. During one period, the instantaneous frequency can be expressed by

$$\omega(t) = \omega_0 + m_\omega(t - t_0). \tag{3.23}$$

The mixing of the transmitting and receiving signals results in

$$u_{\overline{t,r,i}} = \frac{1}{2} A_r A_t \cdot \cos\left(\left(\frac{\omega_0}{c} 2\dot{r} + \frac{2m_{\omega,i}}{c} r\right) t + \phi_{t,r,i}\right), \tag{3.24}$$

a term that is similar to equation (3.22). The circular frequency ($\omega_i,\ i = 1, 2$)

$$\omega_i = \left(\frac{\omega_0}{c} 2\dot{r} + \frac{2m_{\omega,i}}{c} r\right) \tag{3.25}$$

is a linear combination of distance and the relative velocity. Following this, the frequency information is used to determine the distance and relative velocity. This can be achieved by using different slope rates ($m_{\omega,i}$). The FMCW signal in figure 3.4(a) shows a rising slope. Figure 3.5(b) illustrates a (v/s)-plot, it shows the possible range/velocity combi-

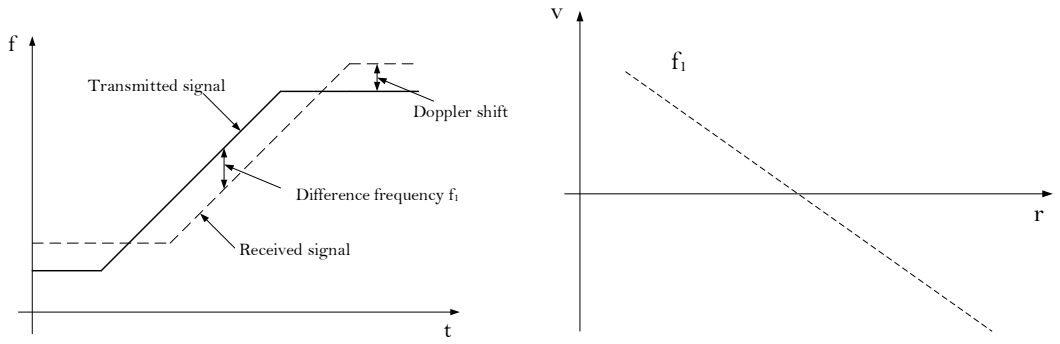

(a) FMCW modulation with positive slope.

(b) Corrosponding distance and realtive velocity values for frequency f_1.

Figure 3.4: FMCW positive slope.

nations for a fixed frequency. The difference frequency will increase when the distance between transmitting and receiving signal rises. This means, the object is moving away from the sensor. Figure 3.5(a) illustrates the increasing difference frequency for a falling slope when the object is approaching the radar sensor. The linear combination of distance and relative velocity of both frequencies is combined in one (v/s) plot shown in figure 3.6. The intersection between both slopes gives the relative velocity and distance

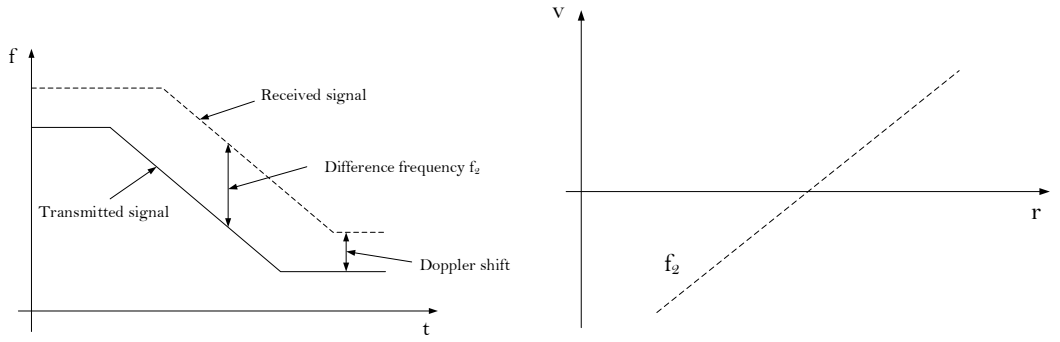

(a) FMCW modulation with negative slope.

(b) Corrosponding distance and realtive velocity values for frequency f_2.

Figure 3.5: FMCW negative slope.

of the object. Following this, equation (3.25) is used to estimate the range by using the circular frequency ω_1

$$\omega_1 = \left(\frac{\omega_0}{c} 2\dot{r} + \frac{2m_{\omega,1}}{c} r \right) \tag{3.26}$$

and ω_2

$$\omega_2 = \left(\frac{\omega_0}{c} 2\dot{r} + \frac{2m_{\omega,2}}{c} r \right). \tag{3.27}$$

Then the range is given by following equation

$$r = \frac{c}{2} \frac{\omega_1 - \omega_2}{m_{\omega,1} - m_{\omega,2}} \tag{3.28}$$

and relative velocity is given by

$$\dot{r} = \frac{c}{2\omega_0} \frac{m_{\omega,1}\omega_2 - m_{\omega,2}\omega_1}{m_{\omega,1} - m_{\omega,2}}. \tag{3.29}$$

FMCW with several frequency slopes is simple to handle, when detecting only one object. More objects can cause detection problems, because the object frequencies ω_i cannot be clearly assigned in the (v/s) plot as shown in figure 3.7. The first two slopes (solid lines) create for two objects four intersection points, where only two are correct (solid circle). To distinguish between several objects more slopes (dashed lines) can be used to identify the correct objects. The intersection point for all four slopes is only valid for two possibilities (solid circle). Guard rails on highways, for example can still cause unwanted multiple detection. Therefore, the equality of the amplitudes is used as an another criteria. The reflected amplitude should be nearly the same size as the emitting amplitude. The object detection is a weak point of the FMCW method [21],[22].

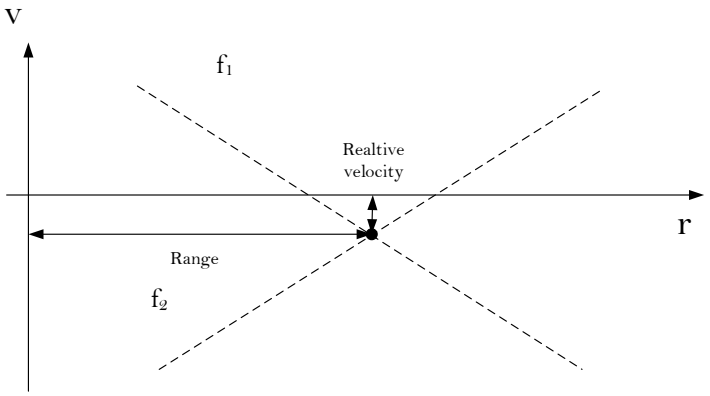

Figure 3.6: Intersection between falling and rising slope f_1 and f_2.

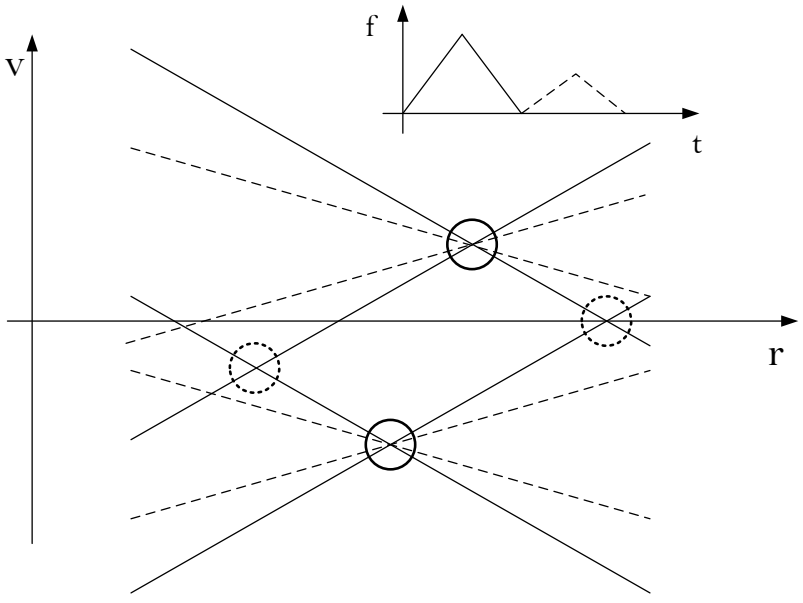

Figure 3.7: FMCW with several frequency slopes.

3.4.3 Frequency Shift Keying (FSK)

Frequency shift keying switches the frequency of the transmitting signal between two distinct frequencies f_1 and f_2 as shown in figure 3.8 [25]. The instantaneous frequency

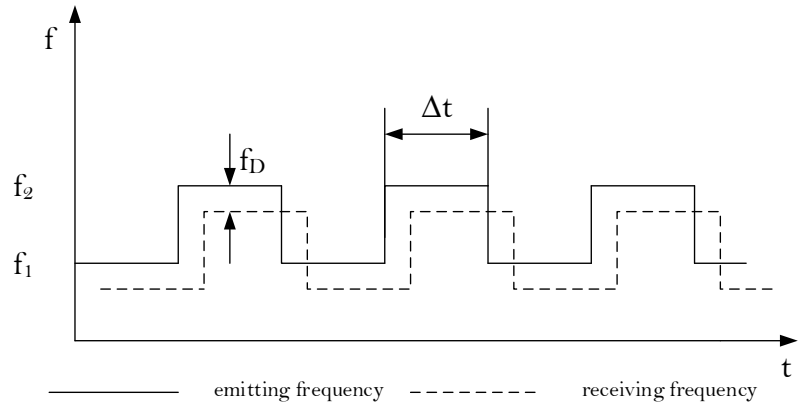

Figure 3.8: FSK emitting and receiving signal.

is modulated by means of a symmetric rectangular signal with a period of $2\Delta t$. The receiving signal is mixed with the carrier frequency. According to equation (3.22), this gives for the frequency f_1

$$u_{\overline{t,r,1}} = \frac{1}{2} A_r A_t \cdot \cos\left(\frac{\omega_1}{c} 2\dot{r}t + \phi_0 - \phi_{r,1}\right), \tag{3.30}$$

and for the frequency f_2

$$u_{\overline{t,r,2}} = \frac{1}{2} A_r A_t \cdot \cos\left(\frac{\omega_2}{c} 2\dot{r}t + \phi_0 - \phi_{r,2}\right). \tag{3.31}$$

For simplification, it is assumed that no Doppler frequency is present. This means, the relative velocity is zero. The phase shift between sending and receiving signal for f_1 is

$$\Delta\phi_{r,1} = \phi_0 - \phi_{r,1} = t_{RT}\omega_1 = \frac{2r}{c}\omega_1, \tag{3.32}$$

where t_{RT} is the time of flight. The phase shift between sending and receiving signal for f_2 is

$$\Delta\phi_{r,2} = \phi_0 - \phi_{r,2} = t_{RT}\omega_2 = \frac{2r}{c}\omega_2. \tag{3.33}$$

The phase difference between the two signals is

$$\Delta\phi_{2,1} = \Delta\phi_{r,2} - \Delta\phi_{r,1} = t_{RT}\Delta\omega, \tag{3.34}$$

where $\Delta\omega$ is

$$\Delta\omega = \omega_2 - \omega_1. \tag{3.35}$$

This can be rewritten to

$$\Delta\phi_{2,1} = \Delta\phi_{r,2} - \Delta\phi_{r,1} = \frac{4\pi r}{c}\Delta f. \tag{3.36}$$

To avoid ambiguity, the phase difference $\Delta\phi_{2,1}$ has to be smaller than 2π. The maximum range is limited to

$$r_{max} = \frac{c}{2\Delta f}. \tag{3.37}$$

The measurement of the phase shift $\Delta\phi_{2,1}$, yields to a target range of

$$r = \frac{c\Delta\phi_{2,1}}{4\pi\Delta f}. \tag{3.38}$$

This can be rewritten to

$$r = r_{max}\frac{\Delta\phi_{2,1}}{2\pi}. \tag{3.39}$$

Until now it was assumed that the target is not moving, hence the estimated phase difference depends only on the distance between sensor and target [23]. The phase shift for moving objects is an overlay of the phase shift between transmitting and receiving signal and the phase difference that is caused by the Doppler frequency. This results in

$$\Delta\phi_{r,1} = r\frac{4\pi f_1}{c_0} + 2\pi f_{D1}t, \tag{3.40}$$

and

$$\Delta\phi_{r,2} = r\frac{4\pi f_2}{c_0} + 2\pi f_{D2}t. \tag{3.41}$$

The Doppler frequencies ($f_{Di},\ i = 1, 2$)

$$f_{D1} = \frac{-f_1}{c}2\dot{r}, \tag{3.42}$$

and

$$f_{D2} = \frac{-f_2}{c}2\dot{r} \tag{3.43}$$

depend linearly to the carrier frequencies ($f_i,\ i = 1, 2$). In order to achieve meaning distances, the carrier frequencies f_1, f_2 should differ from each other slightly. In general the carrier frequency is by several order of magnitude higher with respect to Δf. This means

$$\Delta f << f_1 \quad \text{or} \quad \Delta f << f_2 \tag{3.44}$$

and it can be assumed that the Doppler frequencies f_1 and f_2 are about the same size.

The distance $0 - r_{max}$ can be determined within the region of $0 - 2\pi$. The Doppler frequency can be neglected in equation (3.36), because the phase shift caused by the

Doppler frequency is small compared to the phase shift that is cause by the distance. The impact of moving objects in determining the absolute distance can be neglected. Objects can be detected by their Doppler frequency, but the algebraic sign of the Doppler frequency is not known and has to be estimated by using the phase difference. When the phase difference is rising, the algebraic sign of the Doppler frequency is positive, the object is moving away. A negative Doppler frequency results in an approaching object [22].

3.5 Horizontal Angular Measurement

Besides the measurement of distance and velocity, the azimuth angle/direction of the target is also needed. The angle measurement is done by using focused antenna beams. The elevation angle is is neglected in automotive applications such as adaptive cruise control (ACC), because it is not required [21]. In order to detect a target, the object has to be in within the antenna beam. Angular resolution is the minimum angular separation at which two equal targets can be separated at the same range. The angular resolution characteristics of a radar are determined by the antenna beam width represented by the angle θ which is defined by the half-power (-3 dB) points. The half-power points of the antenna radiation pattern are normally specified as the limits of the antenna beam width for the purpose of defining angular resolution. Two identical targets at the same distance cannot be separated, if they are within the -3 dB beam width of the antenna. This section will explain the mono pulse principle and mechanical or electronic beam pivoting. The width of these lobes and thus the directivity of the antenna is given by the aperture. The choice of the beam width depends on the application. ACC Systems are using narrow lobes and sensors for environment recognition width lobes [24],[26].

3.5.1 Scanning Method

The scanning method in figure 3.9 uses a mechanical or electrical pivoting antenna. Within one measurement cycle, the antenna sweeps over the whole detection range. The beam sweeps in certain angular steps, depending on the design, over the detection range [21]. The scan movement is continuous and the measurements are assigned to discrete angular positions, in particular the center of the actual measurement window. The advantage of the scanning method is the high accuracy and the ability to distinguish between objects regarding to their angular position.

The electronic counterpart to a mechanical scanning method is the phased array antenna. The antenna uses phase shifters to steer the radar beam electronically over the scan sector. When all the phase shifters of the array are properly aligned, the array produces a main beam in the desired pointing direction [27].

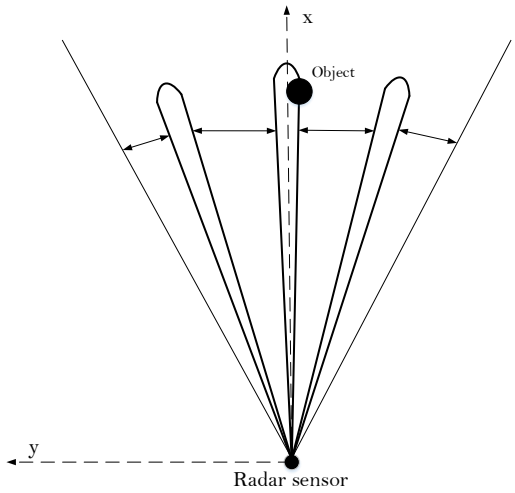

Figure 3.9: Scanning principle.

3.5.2 Mono Pulse Principle

Mono pulse is a method that uses only one radar sensor for the angle measurement. The sensor has more than one antenna. The signals are measured simultaneously and can be processed by using the amplitude comparison mono pulse or the phase comparison mono pulse. The information out of this two methods leads to the target angle. The mono pulse principle can be described on two antennas having complex receiving patterns A and B.

Amplitude Comparison Mono Pulse

The amplitude mono pulse uses uses two overlapping antenna beams, so that the radiation patterns A and B will have slightly different directions [4]. This is shown in figure 3.10. Due to the direction of the antenna beams, the receiving amplitudes for A and B will differ from each other, if the target is not in the center between the two beams. This feature is used to determine the azimuth angle of the object. By using the ratio between difference term and sum term (Δ, Σ) [26]

$$\epsilon(\varphi) = \frac{|\Delta|}{|\Sigma|}, \tag{3.45}$$

where

$$\Sigma = A + B \tag{3.46}$$

and

$$\Delta = A - B. \tag{3.47}$$

This technique is preferred for long range radars with a small coverage angle.

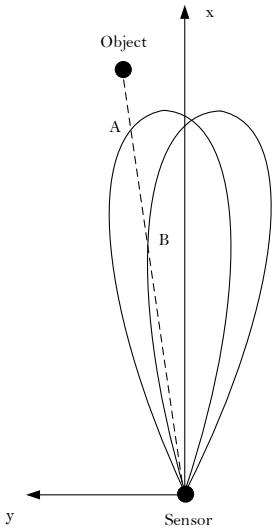

Figure 3.10: Amplitude comparison mono pulse.

Phase Comparison Mono Pulse

The ratio between the difference term and sum term is also used by the phase mono pulse [4], [26]. This method is using tightly aligned receiving antennas with the same receiving pattern as shown in figure 3.11. The distance between the antennas is d, as shown in figure 3.11. The phase difference $\Delta\phi$ for an incideint plane wave is

$$\Delta\phi = d \cdot \sin(\varphi)\frac{2\pi}{\lambda}, \tag{3.48}$$

where $\lambda = c/f_0$ is the wavelength, that is related to the carrier frequency f_0. If the

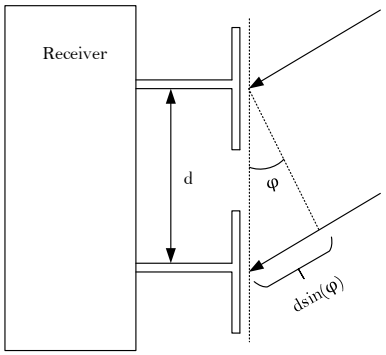

Figure 3.11: Antenna array in receive mode.

antenna patterns A and B are equal, only the phase difference can be used to determine the azimuth angle [4]. In this case the ratio ϵ becomes

$$\epsilon = \frac{\Delta}{\Sigma} = \frac{1 - e^{i\Delta\phi}}{1 + e^{i\Delta\phi}}. \tag{3.49}$$

The phase mono pulse method determines the phase difference $\Delta\phi$, in order to avoid the amplitude calibration, which is required in the amplitude mono pulse method. The angle of direction is obtained by rewriting equation (3.48) to

$$\varphi = \sin^{-1}\left(\frac{\lambda\Delta\phi}{2\pi d}\right). \tag{3.50}$$

4 Radar Simulation

4.1 Introduction

In this chapter the implementation of the radar simulation will be discussed. The radar model in this thesis is a physical approach to a radar simulation, which operates on the principle of geometrical optics. Figure 4.1 illustrates the entire radar simulation environment. The radar physics (radar equation, wave propagation, antenna gain) from previous chapters are considered in this radar simulation. The input of the radar simulation is a traffic scenario and the output is an object list, which provides data of the input scene, as seen by the radar sensor. Figure 4.1 depicts the steps to generate this list. To identify seen objects a block called radar simulation is used. Velocity information is extracted from the input data.

Literature [2], [24] states simple geometric radar models, which only rely on the scene. A simple radar sensor model for example calculates the closest point of the object to the

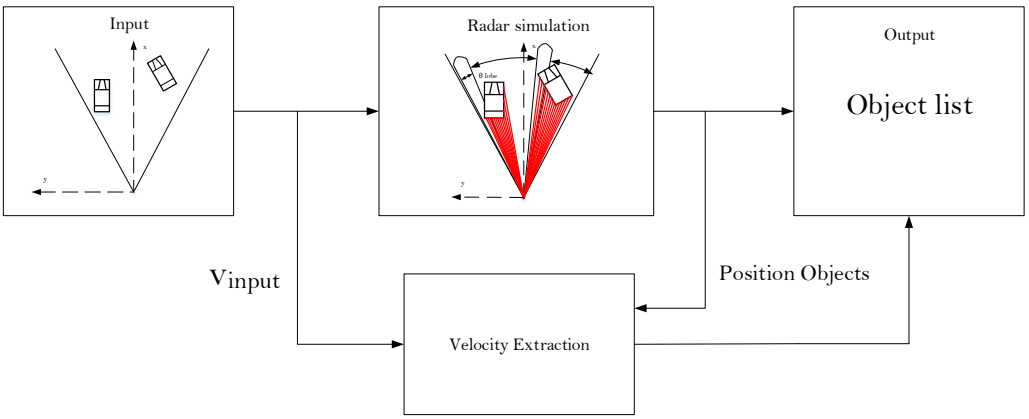

Figure 4.1: Radar simulation overview.

sensor as shown in figure 4.2(a). If the object is located inside of the sensors field of view, even partially, the nearest point corresponds to the nearest located point of the detected object. This could be a point along the object surface or a corner . Another simulation approach is the use of pre defined marking points on the objects. This method selects

the nearest active marking point shown in figure 4.2(b). This kind of radar models are very fast to implement. These models do not consider the specifiecs of a radar. To make the simulation more realistic, non ideal behaviour of the system is incorporated. E.g. receiver operator curves are incorporated to deteriorate the behaviour.

The simulation approach in this work is able to determine a radar signal, which is based on the radar system specifics. This model can deal with complex traffic scenarios and subsequently it is able to distinguish between several vehicles in one field of view (FOV) of the radar sensor.

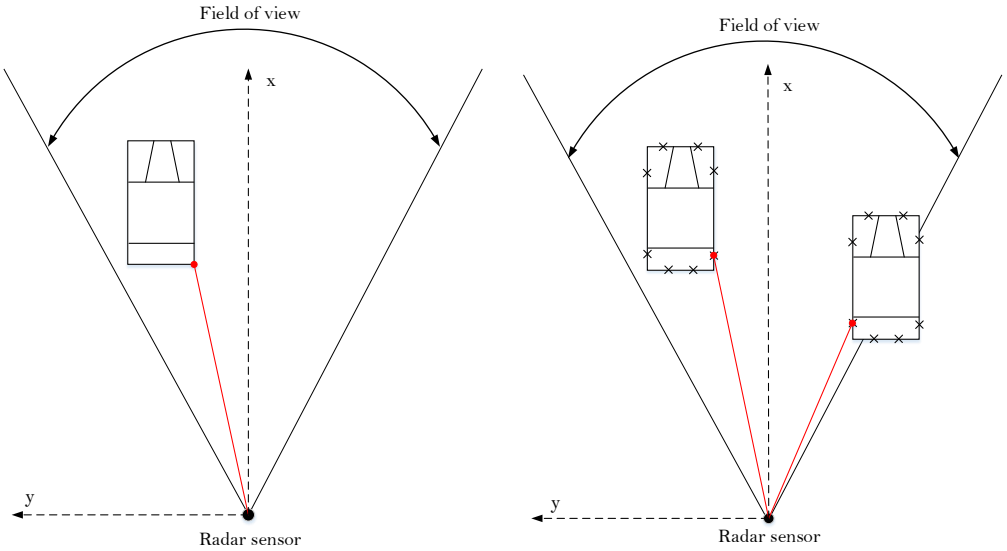

(a) Radar model nearest point.

(b) Radar model using pre defined marking points.

Figure 4.2: Radar model examples without radar specifics.

4.2 Model Structure/Properties

Figure 4.3 shows the processing steps of the radar model . The input for the radar model is provided by the simulation tool (Carmaker/Simulink). The input gives the coordinates of the objects, which are located in the sensor based coordinate system. There are three coordinate systems:

- Inertial coordinate system is used as a global reference system. In this system the vehicle movements are described in relation to the global reference system.
- Vehicle based coordinate system is based on a fix vehicle reference point.

- Sensor based coordinate system is needed for environmental recognition. The point of origin of the coordinates is the radar sensor.

The sensor based coordinate system is only used in this radar simulation. The vehicle/objects are modelled by means of rectangles as illustrated in figure 4.4. The outline of each rectangle is parametrized by the coordinates P1, P2, P3 and P4 in cartesian coordinates as shown in figure 4.4.

The radar model is built up modular into four parts:

- Ray tracer
- Antenna characteristics
- Radar signal processing
- Object data

The simulation starts with a geometrical estimation of targets/intersection points for every object (Module: Ray tracer). This is combined with the antenna characteristics of the radar sensor to incorporate the blurring effect of the antenna characteristics. This leads to the radar signal of the object by using the radar equation (Module: Antenna characteristics).

The radar signal leads is provided to the next module of the simulation, the radar signal processing. Basic signal processing algorithms estimate the number of objects, that can be recovered from the radar signal (Module: Radar signal processing). The last block creates a high level feature extraction of the information for further simulations steps (Object data). The output of the radar simulation contains information of the distance R, the horizontal angle φ and the relative velocity v of the objects, as seen by the sensor.

This radar model is an physical approach to radar simulation, which can be adjusted by several radar system parameters.

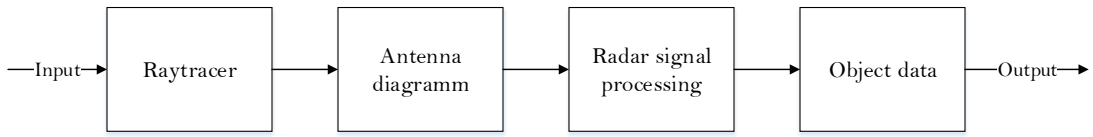

Figure 4.3: Processing steps.

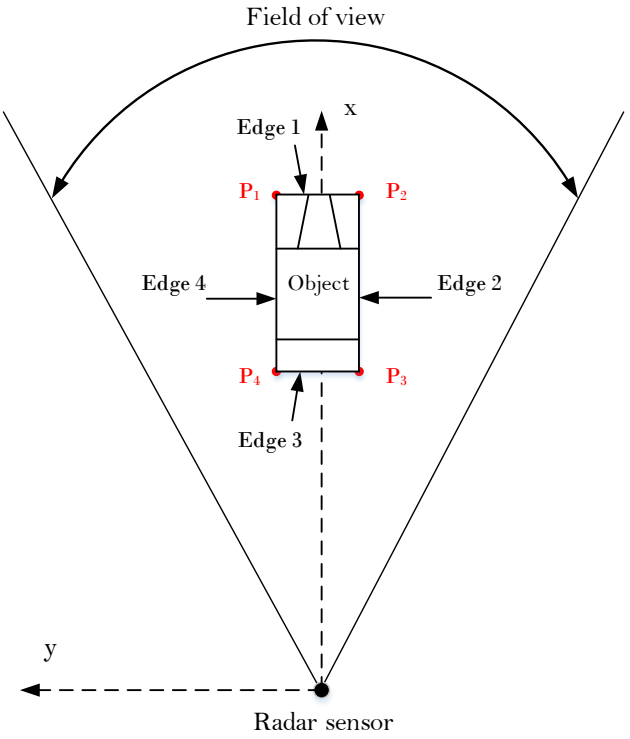

Figure 4.4: Input coordinates P1-P4.

4.3 Ray Tracer

Following section 2.5, the laws of geometical optics can be applied, if

$$\frac{\lambda}{d_{\text{obj}}} << 1 \tag{4.1}$$

holds, where d_{obj} is the dimension of an object. This is given due to the geometry of the object and the frequency of the radar system to be simulated. In conclusion to the previous statement, the behaviour of an electromagnetic waves can be modelled as a ray. The ray tracer is a method to capture the geometric shapes of the object. The basic principle of the ray tracer is, to determine the target point of each ray that impinges on an object. Figure 4.5 illustrates the ray tracing principle. Target points mark reflection points on the edges of the objects that are in the field of view of the radar sensor. The ray tracer scans the whole field of view in one cycle for every object. Possible target points depend on the alignment of the object and the ray tracer step size $\Delta\varphi$, as shown in figure 4.6(a). Detailed implementation steps will be explained in the following subsections.

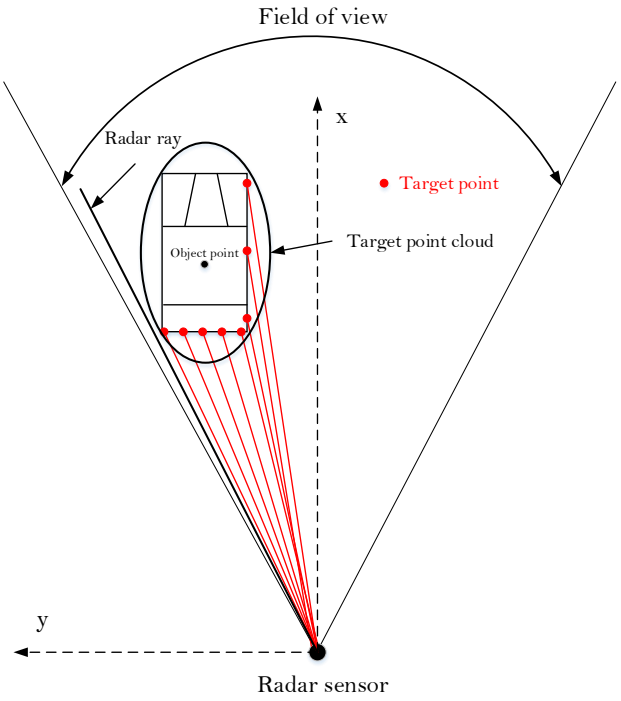

Figure 4.5: Ray tracing example.

4.3.1 Implementation of the Impinging Ray

In order to compute the target points for each object, every target point of a ray that hits the object has to be computed. The object is of rectangular shape. Following this, the object, which illustrates a vehicle is being scanned for every step φ_i in the field of view of the radar sensor. The ray tracer sweeps in φ_N steps from the start to the end of the detection range of the radar sensor shown in figure 4.6(a). If a ray impinges on the object, that is in the field of view of the simulation, the ray tracer will determine a target point. This target point gives the distance to the radar sensor in polar coordinates. This algorithm determines the target/intersection point for every edge of the object and as shown in figure 4.6(b). The state chart in figure 4.7 explains the basic ray tracer algorithm. The object information is given by the input for the simulation. The algorithm in the implementation of this work takes one ray tracer sweep for each object. The condition that must be met for the ray tracer to start is, that the object needs to be in the field of view of the sensor. If the object is in the field of view, the ray tracer will start otherwise it will step to the next object. The ray tracer will run the whole field of view and calculate the intersection points for every object and at every step φ_i. The intersection point/target point will be stored in an array for further processing steps. The intersection point is valid when the radar ray is within the limits of the rectangular object. The limit for the line segment between the coordinate P1 and

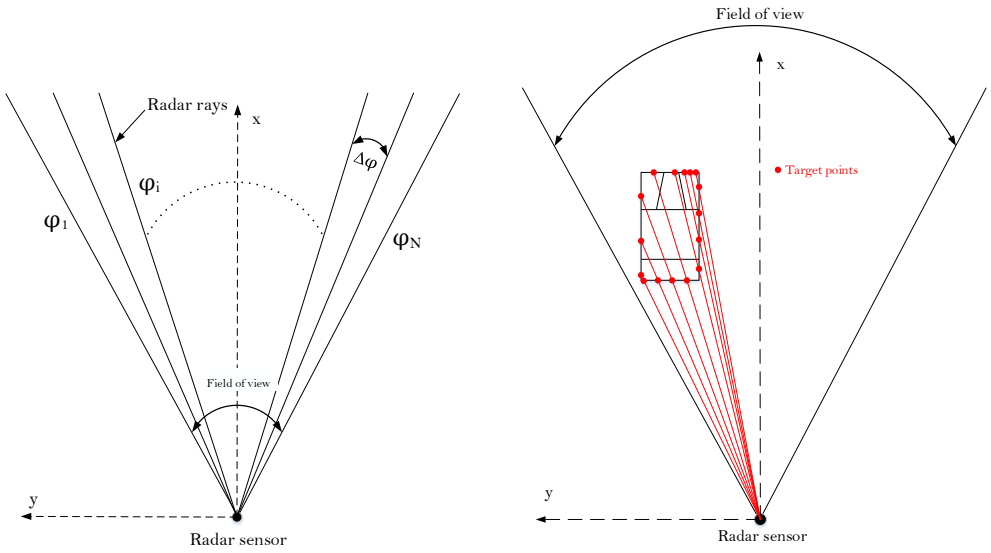

(a) Ray tracer steps.

(b) Basic ray tracer.

Figure 4.6: Basic ray tracer.

P2 is

$$\left(\overline{P1P2}_{x_{min}} \leq x_{ip} \wedge \overline{P1P2}_{x_{max}} \geq x_{ip}\right) \wedge \left(\overline{P1P2}_{y_{min}} \leq y_{ip} \wedge \overline{P1P2}_{y_{max}} \geq y_{ip}\right), \quad (4.2)$$

for P2 and P3, which represents "Edge 2", the limit is

$$\left(\overline{P2P3}_{x_{min}} \leq x_{ip} \wedge \overline{P2P3}_{x_{max}} \geq x_{ip}\right) \wedge \left(\overline{P2P3}_{y_{min}} \leq y_{ip} \wedge \overline{P2P3}_{y_{max}} \geq y_{ip}\right), \quad (4.3)$$

for the coordinate P3 and P4, which represents "Edge 3", the limit is

$$\left(\overline{P3P4}_{x_{min}} \leq x_{ip} \wedge \overline{P3P4}_{x_{max}} \geq x_{ip}\right) \wedge \left(\overline{P3P4}_{y_{min}} \leq y_{ip} \wedge \overline{P3P4}_{y_{max}} \geq y_{ip}\right), \quad (4.4)$$

and for the coordinate P4 and P1, which represents "Edge 4", the limit is

$$\left(\overline{P4P1}_{x_{min}} \leq x_{ip} \wedge \overline{P4P1}_{x_{max}} \geq x_{ip}\right) \wedge \left(\overline{P4P1}_{y_{min}} \leq y_{ip} \wedge \overline{P4P1}_{y_{max}} \geq y_{ip}\right). \quad (4.5)$$

Then intersection point in x-direction can be computed by creating the matrices $\mathbf{A}$

$$\mathbf{A} = \begin{bmatrix} P_{1_{x_{rel}}} - P_{2_{x_{rel}}} & P_{1_{y_{rel}}} P_{2_{x_{rel}}} - P_{2_{y_{rel}}} P_{1_{x_{rel}}} \\ -x_{\text{ray}} & 0 \end{bmatrix}, \quad (4.6)$$

and $\mathbf{B}$

$$\mathbf{B} = \begin{bmatrix} P_{2_{y_{rel}}} - P_{1_{y_{rel}}} & P_{1_{x_{rel}}} - P_{2_{x_{rel}}} \\ y_{\text{ray}} & -x_{\text{ray}} \end{bmatrix}, \quad (4.7)$$

where x_{ray} is the maximum sensing distance. The y-direction y_{ray} is computed by

$$y_{\text{ray}} = x_{\text{ray}} \cdot \tan(\alpha), \tag{4.8}$$

where α is defined as

$$\alpha = \text{FOV}/2 - \varphi_i. \tag{4.9}$$

Then x_{Target} can be computed by

$$x_{\text{Target}} = \det\left[\mathbf{A} \cdot \mathbf{B}^{-1}\right]. \tag{4.10}$$

For the computation of y_{Target} the matrices $\mathbf{C}$

$$\mathbf{C} = \begin{bmatrix} P_{1_{y_{rel}}} P_{2_{x_{rel}}} - P_{2_{y_{rel}}} P_{1_{x_{rel}}} & P_{2_{y_{rel}}} - P_{1_{y_{rel}}} \\ 0 & y_{\text{ray}} \end{bmatrix}, \tag{4.11}$$

and $\mathbf{D}$

$$\mathbf{D} = \begin{bmatrix} P_{2_{y_{rel}}} - P_{1_{y_{rel}}} & P_{1_{x_{rel}}} - P_{2_{x_{rel}}} \\ y_{\text{ray}} & -x_{\text{ray}} \end{bmatrix}, \tag{4.12}$$

have to be constructed. Then y_{Target} is given by

$$y_{\text{Target}} = \det\left[\mathbf{C} \cdot \mathbf{D}^{-1}\right]. \tag{4.13}$$

When all ray steps are done, the ray tracer algorithm will end. As the ray tracer detects target points on all corners, further processing is required to clean up the raw data of this processing step.

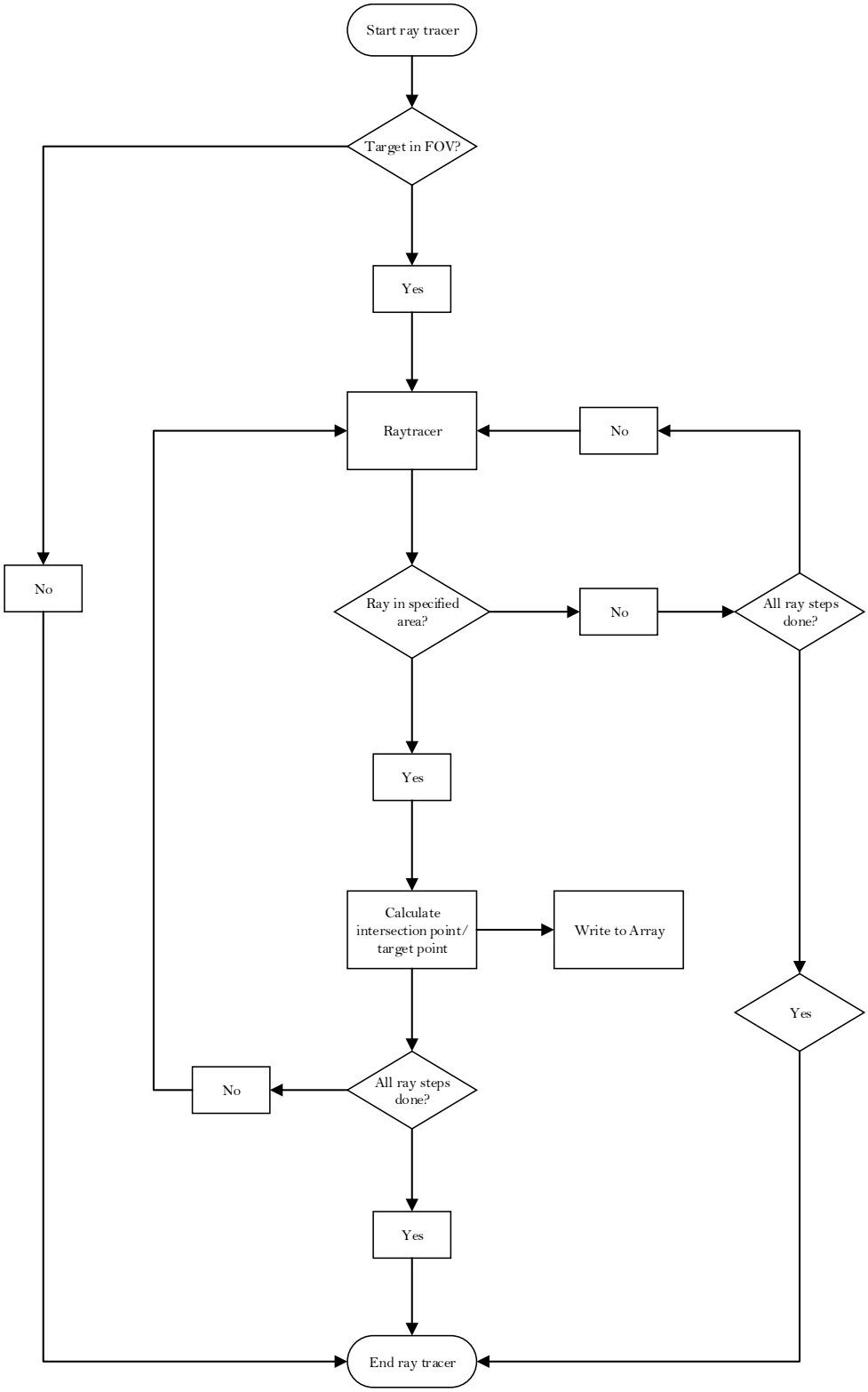

Figure 4.7: Impinging ray algorithm.

4.3.2 Reflecting Edge Detection

The basic ray tracer algorithm in the previous section determines the intersection points for the entire object, as shown in figure 4.6(b). In the next step, the output has to be filtered, to detect target points, that are not concealed by other edges. The edges are defined as shown in figure 4.4. This computation is based on the alignment of the object. Possible orientations of the objects in the field of view is illustrated in figure 4.8. The computational steps are summarized in figure 4.9. An object can have five possible orientations.

If the object is rotated to the left side around its own axis, that means the P_2 x-coordinate is larger than the P_1 x-coordinate, "Edge 3" and "Edge 4" will be selected as shown in figure 4.8(b). Logical checks of the corner coordinates can be done with the help of figure 4.8 to evaluate other object alignments and corresponding reflecting edges.

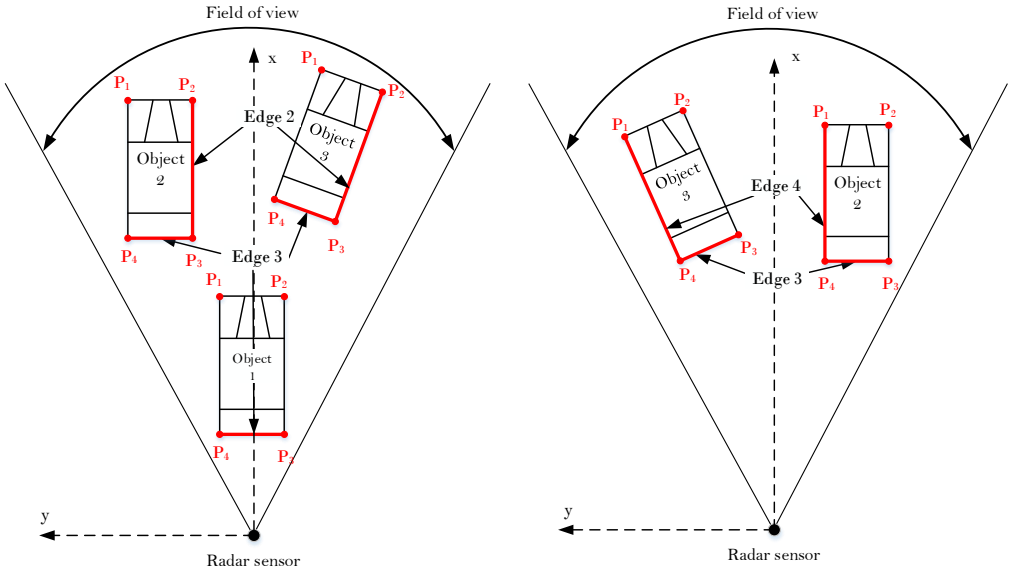

(a) Active edge alignment 1.

(b) Active edge alignment 2.

Figure 4.8: Possible active edge alignments.

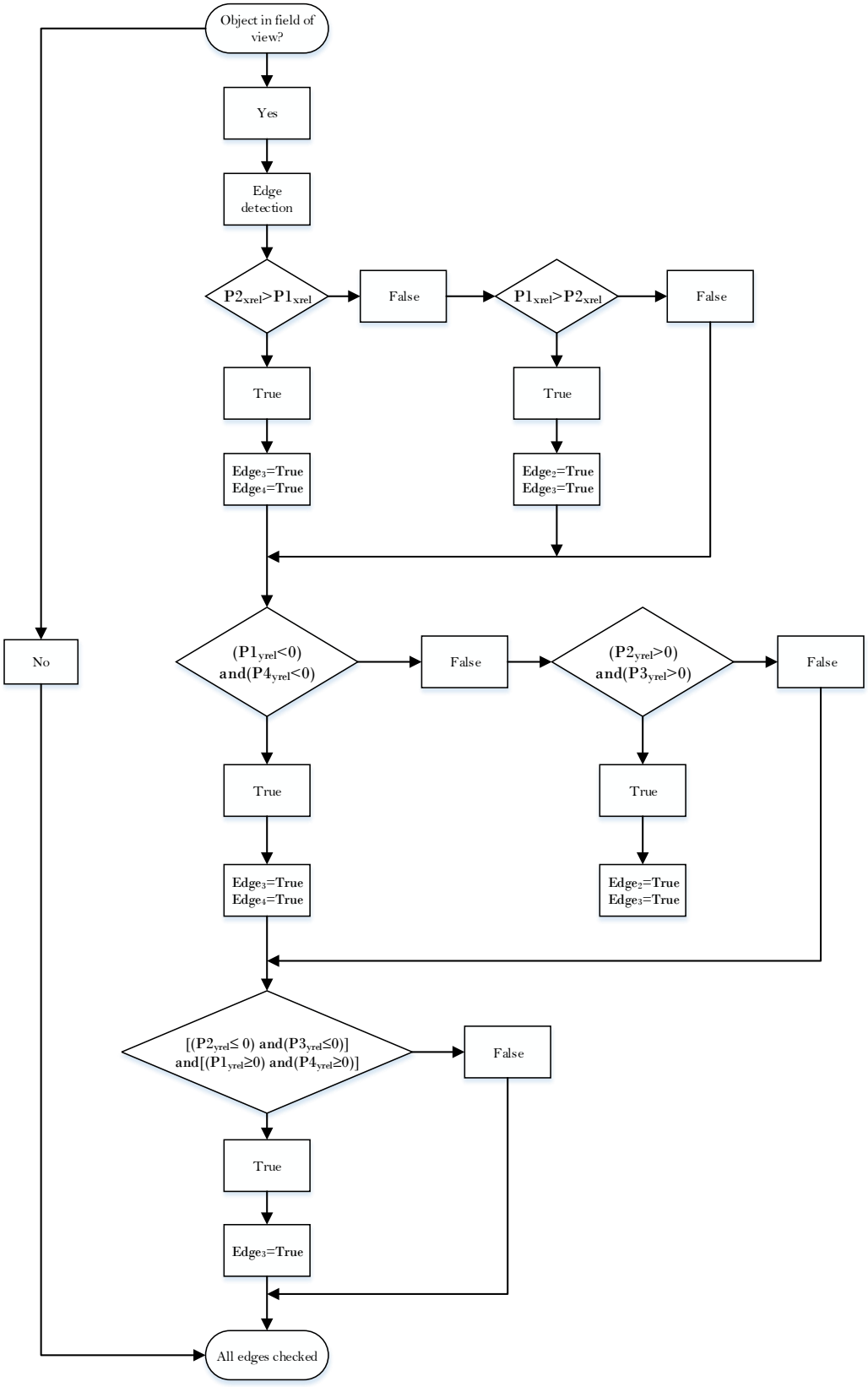

Figure 4.9: Edge detection algorithm.

4.3.3 Object Coverage

In the previous computation step, the raw output of the ray tracer was filterd to remove data from self covered edges. Yet, also different objects can lead to covering as shown in 4.10. The radar sensor can only see objects in its line of sight. In figure 4.10 the object 1 is fully overlapped with object 2 and this will result in disabling all target points at object 1. This means, that the object 1 is not seen at this traffic scenario by the radar sensor model. The simulation searches for the first impinging ray. The two passing rays between object 1 and object 2 are the closest non hitting object rays. This means, that the ray tracer step φ_i is at a position, where no target point can be calculated. Object 3 is directly visible and all target points, which hit the object can be enabled. The radar sensor model will only see at this traffic scenario object 2 and object 3 now.

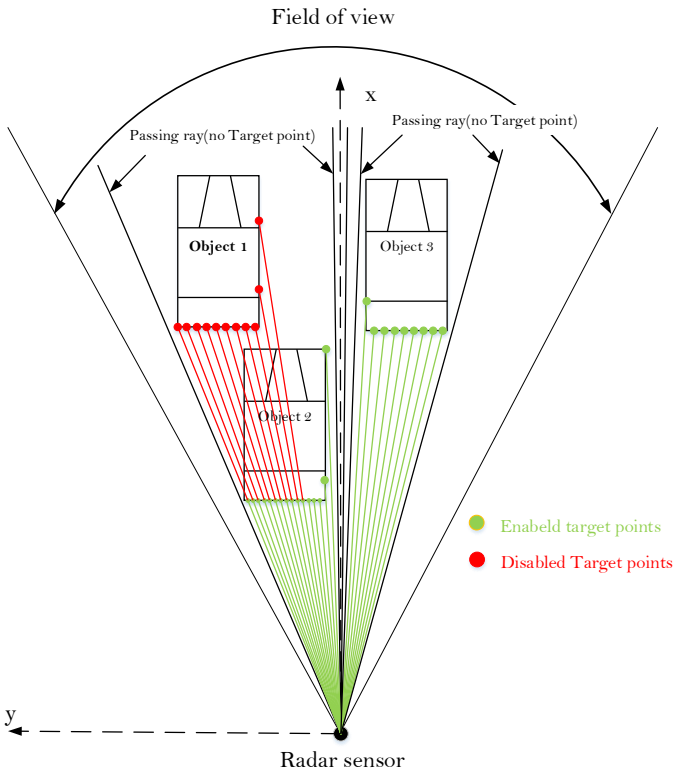

Figure 4.10: Illustration of Object coverage.

4.3.4 Final Ray Tracer

The final ray tracer combines the basic ray tracer, edge detection and object overlap together. This final ray tracer can now be used in the further modelling process. Figure 4.11 shows the simulation result for one object in the sensing region and the found

target point as a function of the angle ϕ. Figure 4.12 shows the simulation result for three objects. It can be seen, that the first two objects are over lapping. Thus, the first object is not fully seen. The final ray tracer delivers a scanned map of the objects, that are in the the field of view. By changing the step size $\Delta\varphi$ of the rays, the resolution of the ray tracer can be increased or decreased. The overview of the final ray tracer is shown in figure 4.13.

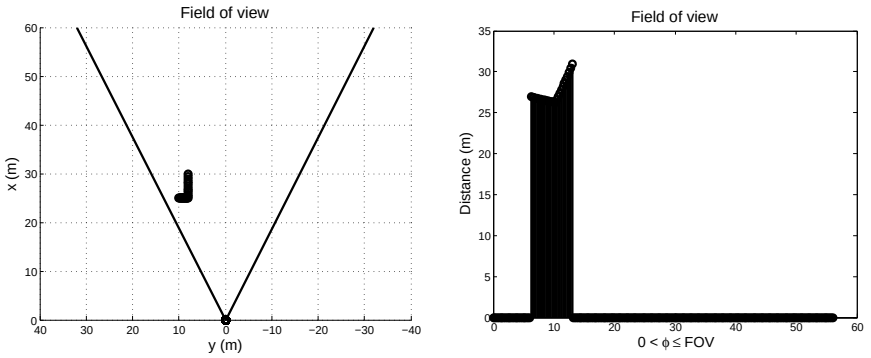

(a) Ray tracer in the sensing region. (b) Distance as a function of the angle ϕ.

Figure 4.11: Simulation result one object.

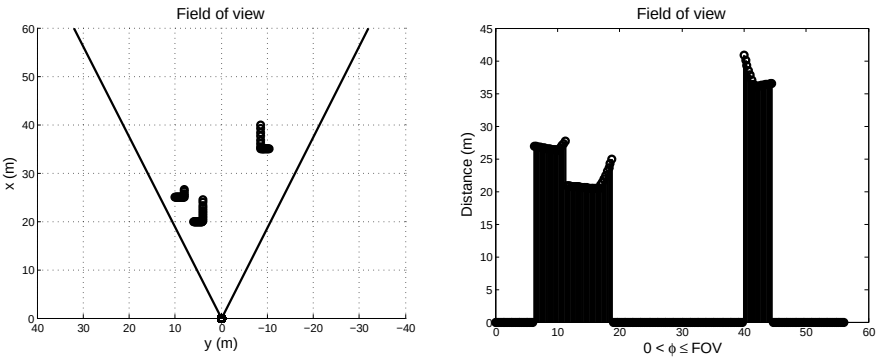

(a) Ray tracer in the sensing region. (b) Distance as a function of the angle ϕ.

Figure 4.12: Simulation result three objects.

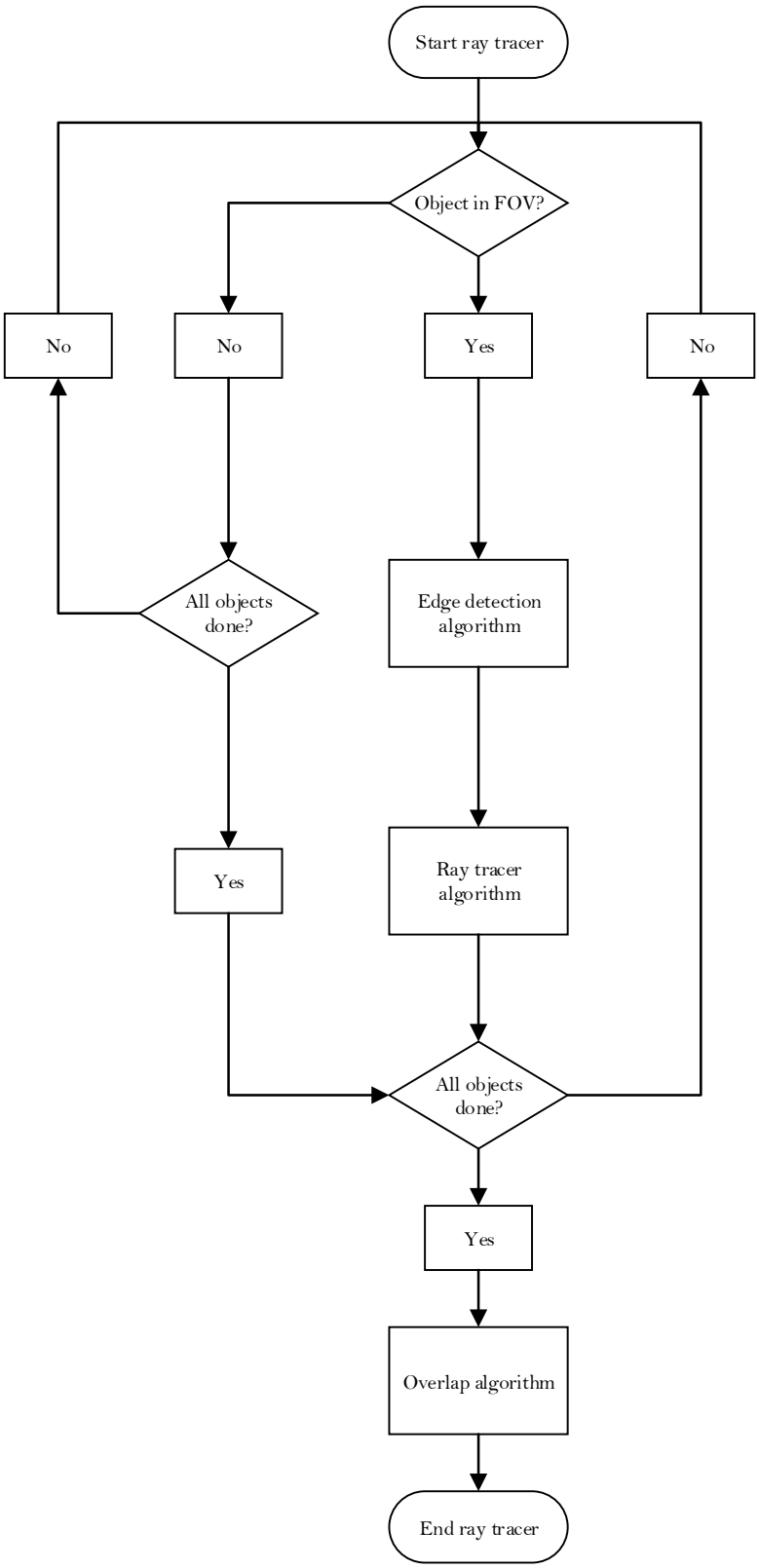

Figure 4.13: Entire ray tracer algorithm.

4.4 Antenna Characteristics

This section will explain the incorporation of the antenna characteristics. A directional antenna emits more power in an certain direction. In chapter 2 the radar equation was introduced under the assumption, that the antenna of the radar is perfectly aligned on the target. In section 3.5 the antenna pattern was explained to cause an angular resolution behaviour of a radar.

Due to the width of the main lobe, a blurring effect occurs, limiting the perfect resolution behaviour computed by the ray tracer. This effect will be incorporated in this section. Figure 4.14 illustrates the basic principle of the incorporation of the antenna characteristics with the main lobe. The antenna characteristics are causing a blurring of the output of the ray tracer. This equals a convolution, between the antenna pattern and the ray tracer information.

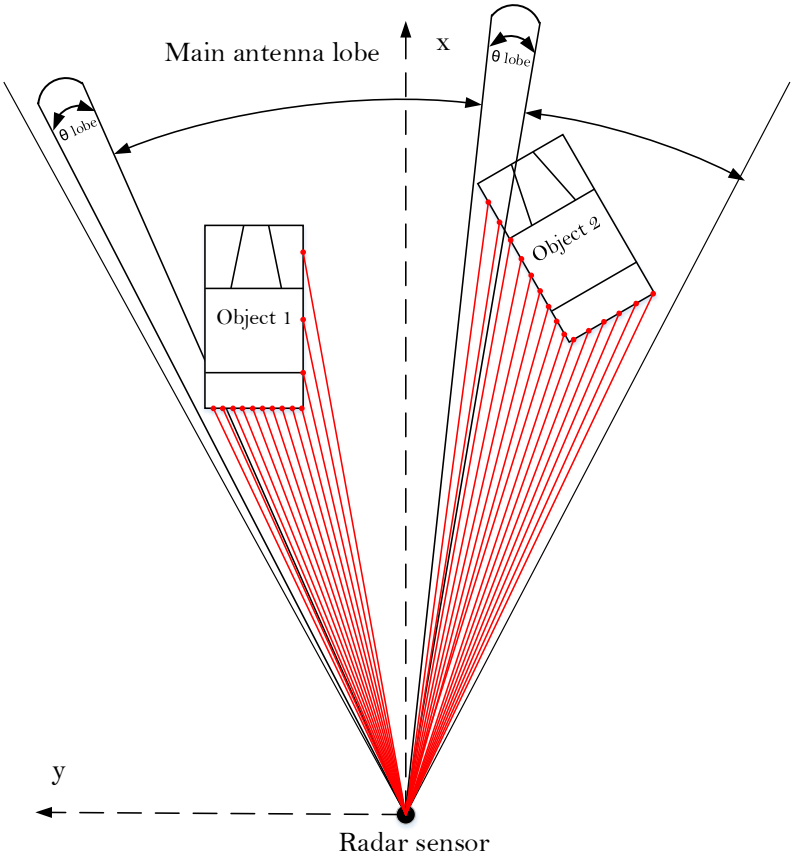

Figure 4.14: Field of view with main antenna lobe.

4.4.1 Antenna Gain

The antenna gain was explained in section 2.4. To incorporate an antenna gain into the simulation, a normalization is required. Figure 4.15 illustrates a gain, as used in this work. A gain parameter K_G has to be determined, such that

$$G_{\text{norm}} = K_G \int G(\phi) d\varphi = 1, \tag{4.14}$$

holds.

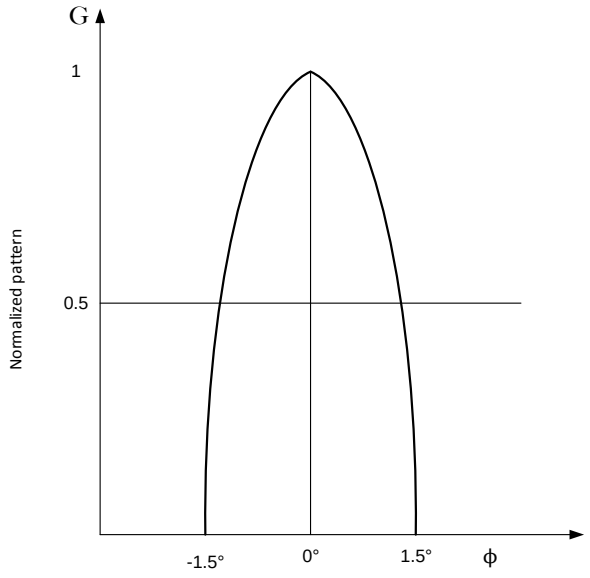

Figure 4.15: Antenna diagram main lobe.

4.4.2 Convolution Algorithm

The output of the ray tracer is to the objects, the distance as a function of ϕ. To incorporate the antenna, this signal has to be convoluted with G_{norm}. Figure 4.16 illustrates the convolution.

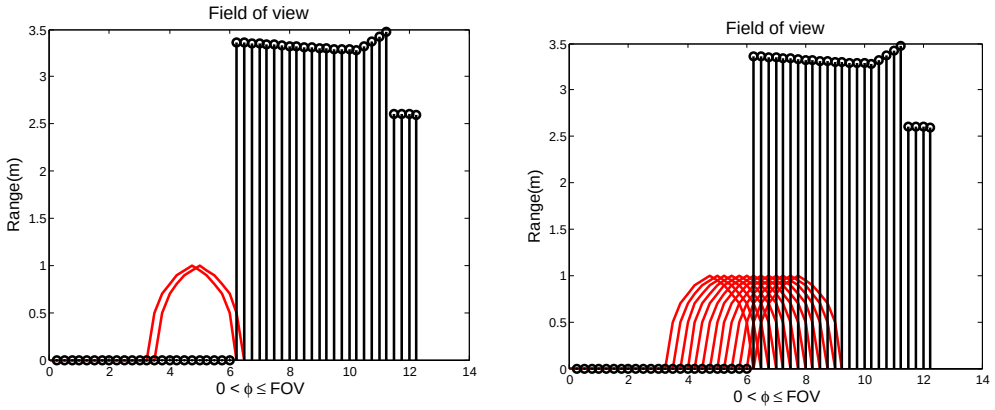

(a) Convolution algorithm 2 steps.

(b) Convolution algorithm n steps.

Figure 4.16: Ray tracer antenna main lobe convolution.

Figure 4.17(b) illustrates the effect of the antenna gain. As can be seen, the antenna characteristics causes a blurring, thus leading to reduced spatial resolution.

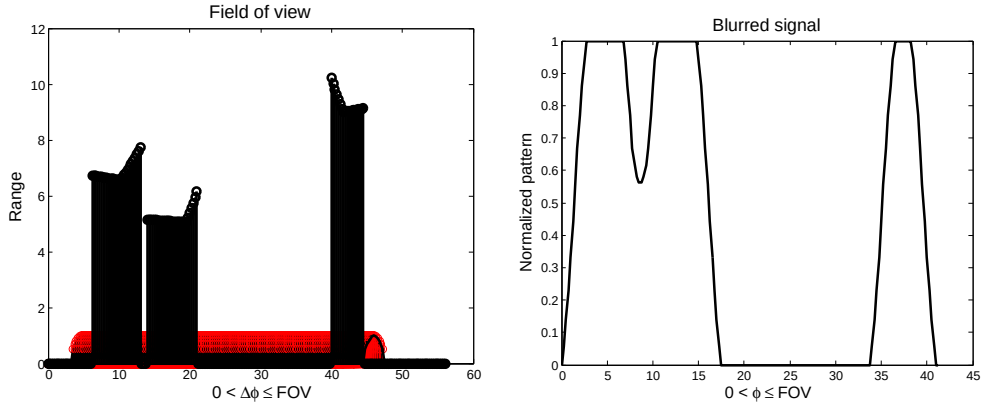

(a) Convolution algorithm last step.

(b) Blurred signal.

Figure 4.17: Ray tracer and antenna main lobe convolution last step for 3 objects.

4.5 Incorporation of the Radar Equation

By now the geometry and the antenna pattern have been incorporated. In a final step to compute the received power, the radar equation has to be included. The computed blurred signal of previous step is multiplied with an power factor K_P to have the effective signal power P_E, which corresponds with the objects in the line of sight of the radar. The received power as function of ϕ as shown in figure 4.18 is calculated by using the the radar equation

$$P_R = \frac{P_E G \sigma A_e}{(4\pi)^2 R^4}. \tag{4.15}$$

The radar equation also allows the incorporation of object properties, e.g. different reflections. After this step, the final radar signal is computed, which can be used to extract information as seen by the radar.

4.5.1 Radar signal-Threshold Level

The obtained signal presents the received power of the sensor. It represents the scenario seen by the radar sensor with several system parameters incorporated. The signal is defined in this work as the radar signal. it is know the task to extract information about the scene from this signal. In order to adjust the simulation for a maximum range of the radar, a initial threshold is applied to remove infeasible data. While this is a simple way to set a maximum range, even this threshold has to be adjusted with car. Figure 4.20(b) illustrates can lead into disappearing some target points in the sensing region.

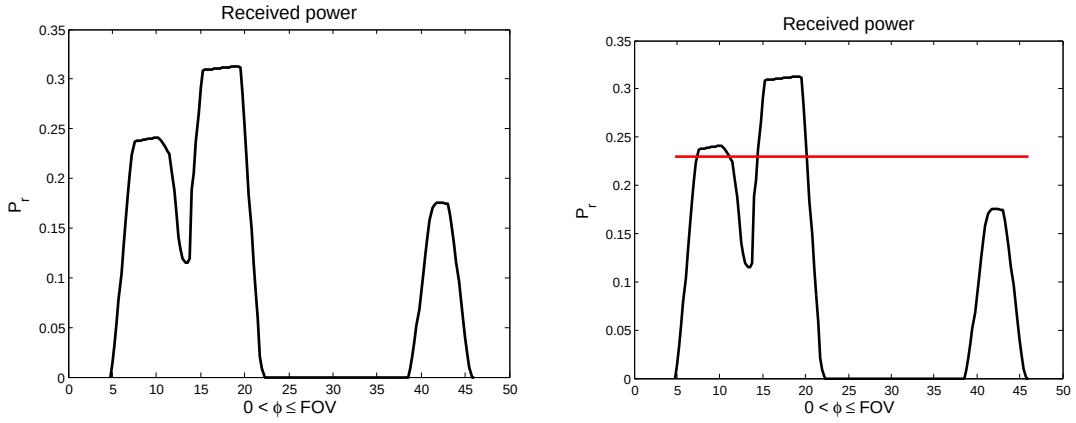

(a) Received power without threshold.

(b) Received power with threshold.

Figure 4.18: Received power/Radar signal as a function of ϕ.

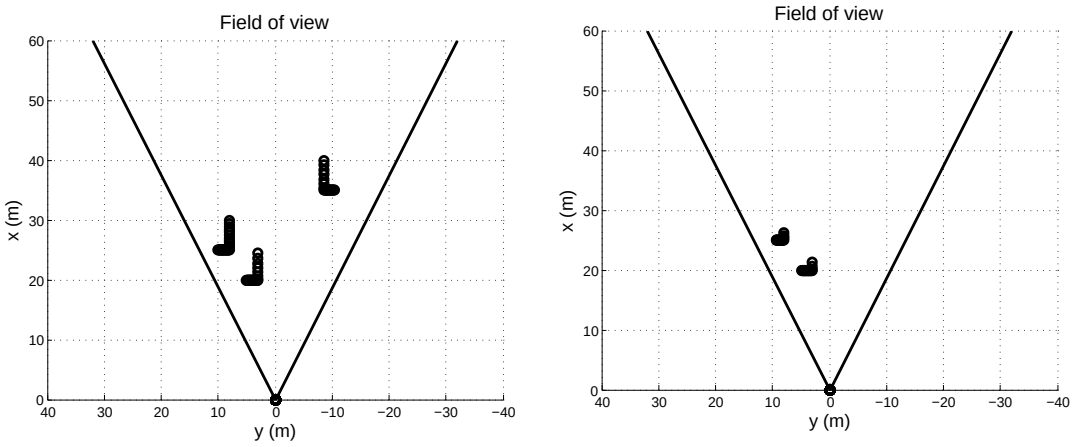

(a) Sensing region without threshold.

(b) Sensing region with threshold.

Figure 4.19: Sensing region with and without threshold for three objects.

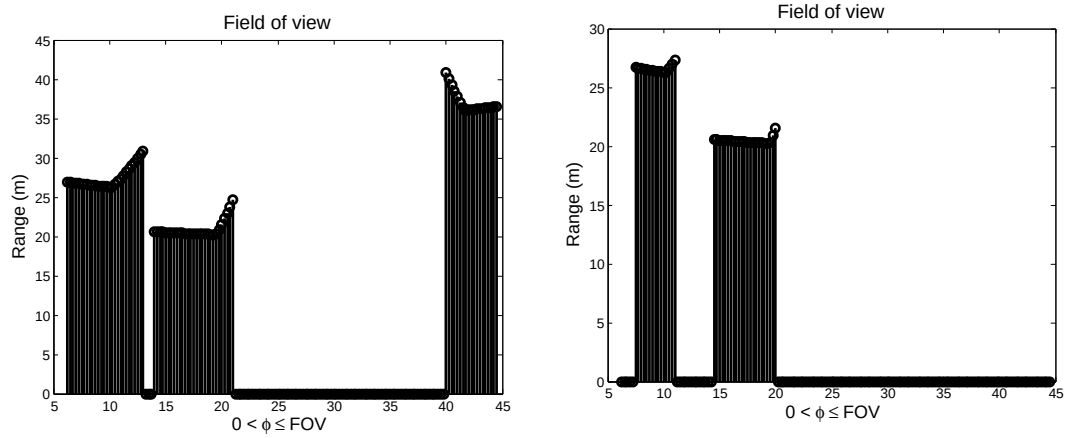

(a) Distance as a function of ϕ without threshold.

(b) Distance as a function of ϕ with threshold.

Figure 4.20: Distance as a function of ϕ with and without threshold for three objects.

4.6 Simple Radar Signal Processing

In this section a simple strategy to recover information is presented. The radar signal is processed to extract the observable information about the scene, in order to generate an object list.

The radar signal processing is divided into three steps:

- Step 1: Object identification without overlap recognition
- Step 2: Object identification with overlap recognition

The strategy will be explained for the three objects scenario as depicted in figure 4.19(a).

4.6.1 Object Identification without Overlap Recognition

Figure 4.21 shows the radar signal of the objects, that are in the field of view of the sensor. Every peak in the plot corresponds to an object. The first step is, to split up the peaks that are not merged together. In the illustration 4.21, the red marking shows, that between the receiving power peaks no power is received. Following this, the objects can be identified when the receiving power drops to a low threshold value between the peaks. The number of objects to be detected in the following example is two.

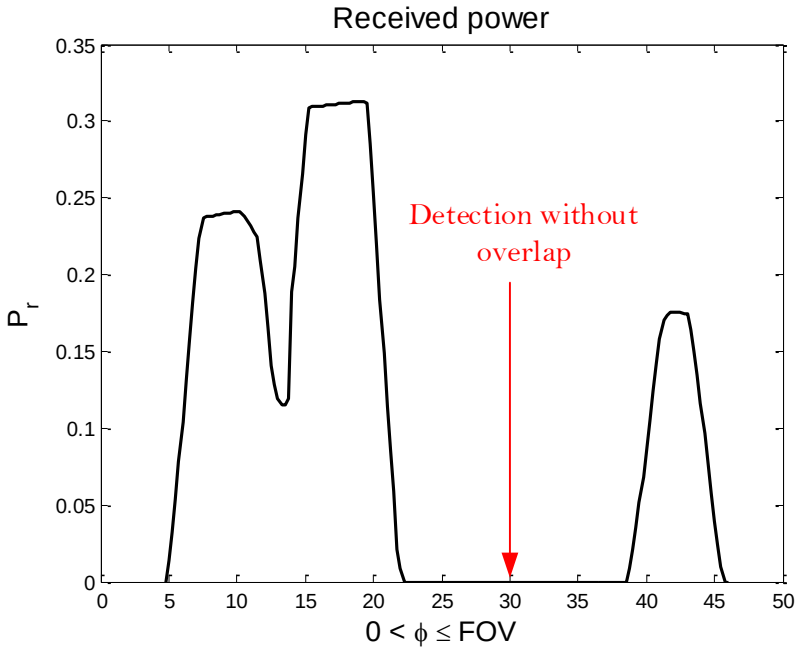

Figure 4.21: Object identification without overlap recognition.

4.6.2 Object Identification with Overlap Recognition

The first step identifies the objects, by means of a certain threshold. The number of objects in step one was two. When objects are close together, they appear to be merged in the radar signal. Hereby, the algorithm has to be adjusted with respect to the SNR.

The first peak in figure 4.22 shows, that the radar signal has a signal drop in between. This can be used as an indication that two objects are merged together. To find more objects an algorithm searches for significant drops in the signal. Figure illustrates 4.22 the signal drop and this is processed by the algorithm, which results for this example in two objects.

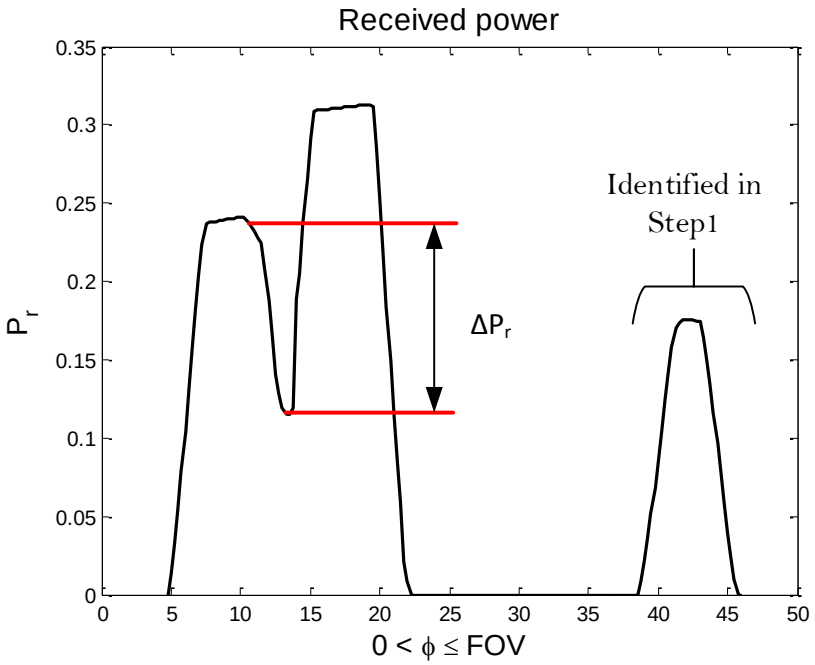

Figure 4.22: Object identification with overlap recognition.

Figure 4.23 depicts the result for the processed radar signal. In this example, all three objects could be found.

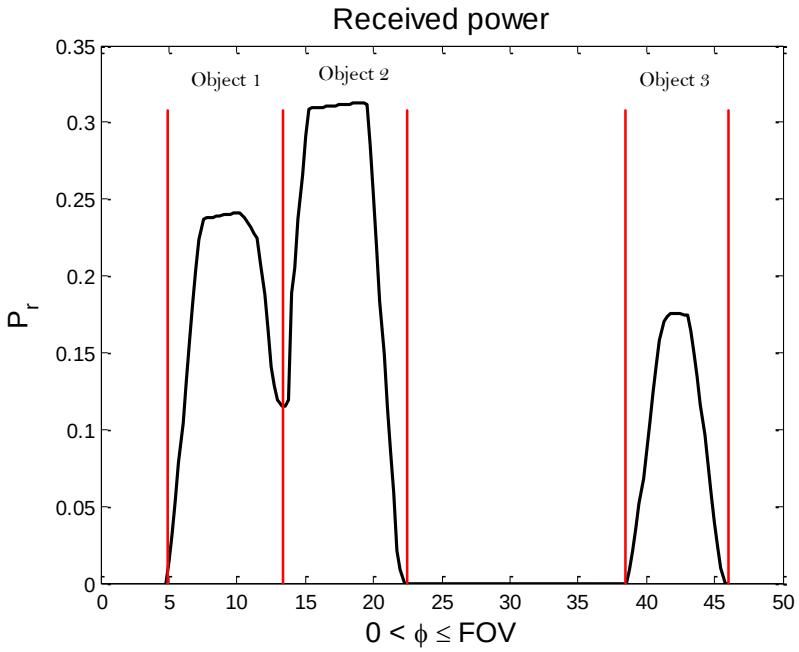

Figure 4.23: Object splitting.

4.7 Creation of Object Data

The last step of the radar simulation is the generation of the object data for each object. The information that the signal processing provides, is merged with the velocity information of the input. Figure 4.24 illustrates the final result.

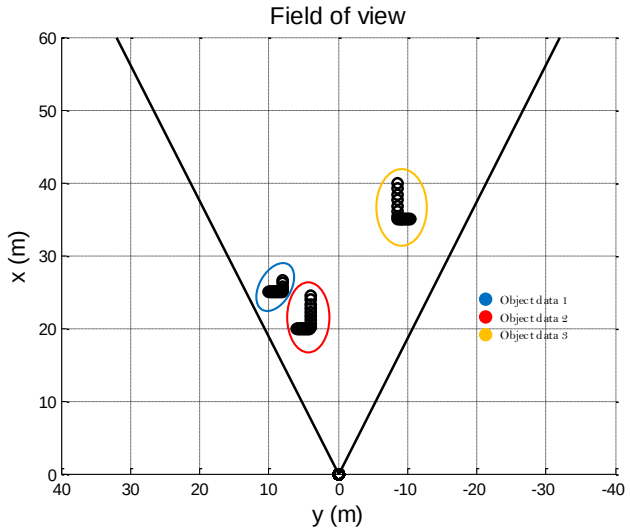

Figure 4.24: Illustration of data points.

4.7.1 Extraction of Meta Data

The object data gives following information:

- Number of objects
- Object dimensions
- Center of mass for every object
- Corresponding azimuth angle
- Corresponding relative velocity

4.7.2 Object Dimensions

The object dimensions can be estimated by fitting a rectangle to the target points of the object. The information of the data points that is available, is used to determine the length and width of the object. An example is shown in figure 4.25. The length/width of one edge is calculated by using the difference of the last target point and the first target point for the x-coordinate

$$\Delta x_{\text{edge},i} = x_{\text{last},i} - x_{\text{first},i}. \tag{4.16}$$

The same is done for the y-coordinate

$$\Delta y_{\text{edge},i} = y_{\text{last},i} - y_{\text{first},i}. \tag{4.17}$$

The length of one edge can now be determined by using

$$l_{\text{edge},i} = \sqrt{\Delta x^2_{\text{edge},i} + \Delta y^2_{\text{edge},i}}. \tag{4.18}$$

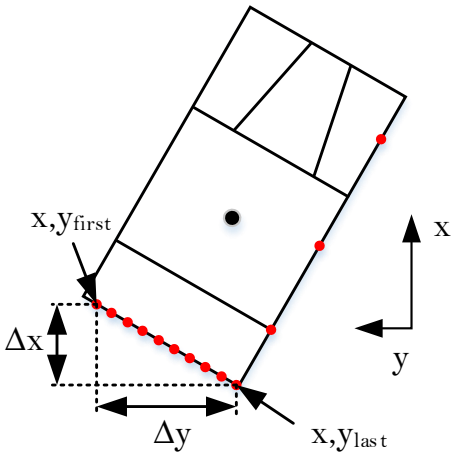

Figure 4.25: Length calculation.

4.7.3 Center of Mass

For driving assistance systems, information about the center of mass can be useful. The center of mass can be determined, by using the position of the first target point in x-direction and y-direction and the last target point in x-direction and y-direction. Figure 4.26 shows an example of the center of mass calculation. The center of mass will change depending on the object alignment. The center of mass is calculated in x-direction by

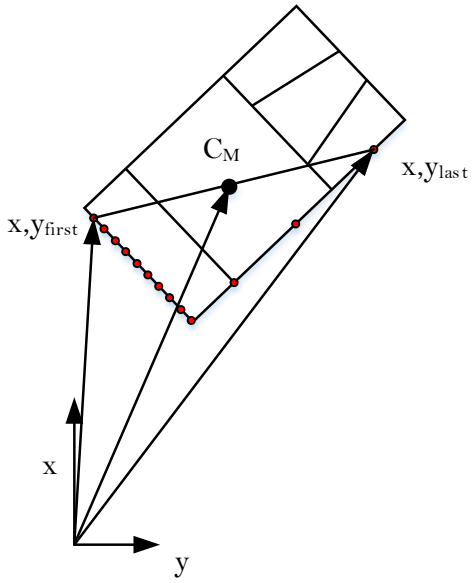

Figure 4.26: Center of mass calculation.

$$C_{M_x} = \frac{x_{\text{first}} + x_{\text{last}}}{2} \tag{4.19}$$

and y-direction by

$$C_{M_y} = \frac{y_{\text{first}} + y_{\text{last}}}{2}. \tag{4.20}$$

This yields to a center of mass in polar coordinates

$$C_M = \sqrt{C_{M_x}^2 + C_{M_y}^2}, \tag{4.21}$$

where the corresponding angle is

$$\varphi_{C_M} = \arcsin\left(\frac{C_{M_y}}{C_M}\right). \tag{4.22}$$

The relative velocity is used from the simulation input and assigned with the corresponding objects from the radar simulator output.

4.8 Simulation Result

Figure 4.27 shows the simulation result without noise. The radar signal, which is at the bottom is ideal. The plot in the upper left is the traffic scenario and the plot to the left is the output signal of the radar simulator. Figure 4.28 shows the simulation with noise. The radar signal, which is at the bottom is corrupted with white noise. It can be seen that the radar simulator output is different compared to the ideal plot. This is due to the radar signal with noise. Further signal processing needs to be done to reconstruct a similar radar signal like in figure 4.28.

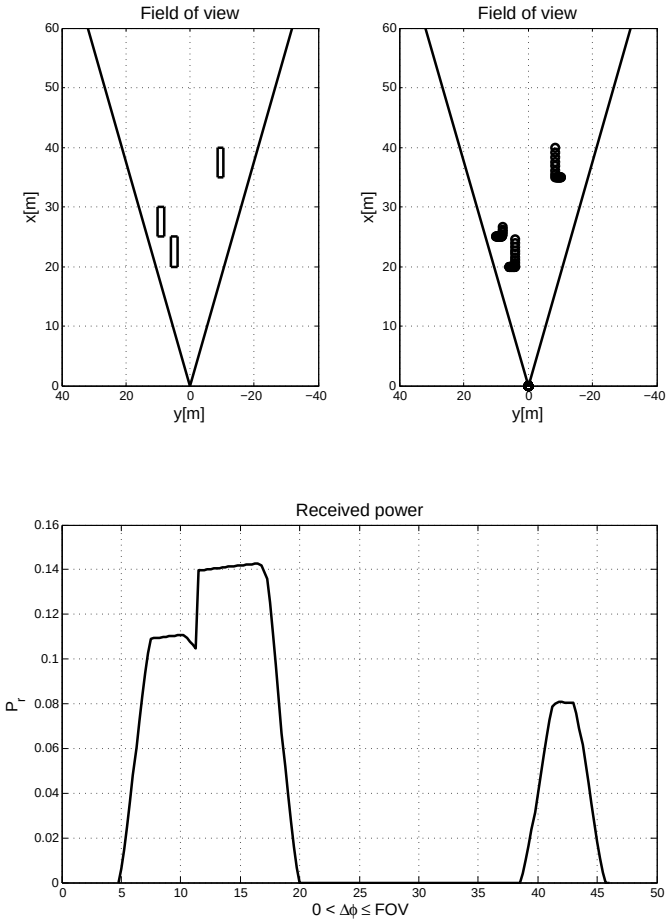

Figure 4.27: Simulation result without noise.

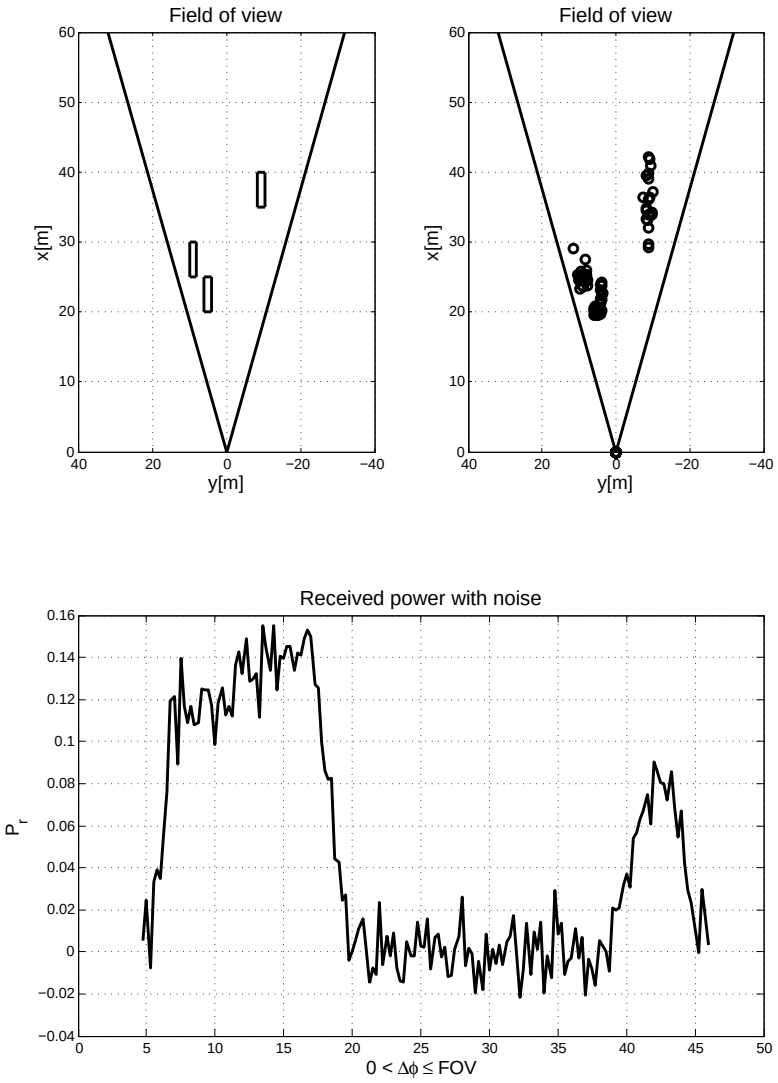

Figure 4.28: Simulation result with noise.

5 Conclusion and Outlook

Radar sensors are used in many automotive applications and above all in driving assistance systems. To make sure such advanced safety systems work properly it is essential to test them. Validating those systems in real traffic is time consuming and can lead to high costs. To speed up the development of advanced assistance systems, virtual driving simulation tools are used. Driving simulators offer a potent virtual prototyping platform to test and verify advanced safety systems in different development phases. Simple geometrical models without radar system specifies are often used to model the radar sensor in simulations tools.

In this thesis a physical based sensor model was developed. The radar simulation a modular design consisting of four parts. The first part is the ray tracer, which follows the laws of geometrical optics. The ray tracer determines reflection points of each ray that encounters the object. The step size of the ray tracer is $\Delta\varphi$, which can be increased or decreased. This yields to a higher or lower scan resolution. The second part considers the antenna characteristics. Due to the main lobe of the antenna, a blurring effect occurs. The blurring effect limits the perfect scan resolution of the ray tracer and can be affected by changing the beam width of the antenna. In a final step the radar signal is generated by using the radar equation. Every object, that is detected by the radar can be afflicted with different radar cross sections, this will lead to a different radar signal. Disturbances can be added, because no receiver is perfect and adding some noise to the signal path results in a different radar signal. The third part is basic radar signal processing and it is used to extract the object information. This part can be advanced to high level signal processing, in order to handle complex radar signals. The last part extracts meta data from the objects. The velocity information of the input is combined with the object data. This radar simulation gives a variety of changeable and parametrizable settings.

The result of this work is a concept to a generic radar model, which is individually adjustable by the characteristics of a radar system. A next step in the implementation could be target tracking. This model is an addition to current radar models and because of the ray tracing approach it is suitable for complex traffic scenarios. The model could be used in future in driving simulation tools.

List of Figures

Bibliography

[1] Hermann Rohling Florian Fölster. Signal processing structure for automotive radar. 2006.

[2] *IPG Automotiv GmbH: CarMaker Reference Manual Version 3.5.4, Reference Manual, 2012.*

[3] Carsten Brenk Jürgen Dickmann, Nils Appenrodt. Der beitrag von radarsenradar zum autonomen fahren. *Automobil Elektronik*, 2014.

[4] V. Issakov. *Microwave Circuits for 24 GHz Automotive Radar in Silicon-based Technologies.* Springer Berlin Heidelberg, 2010.

[5] A.G. Stove. A software simulator for automotive radar. In *Computer Modelling and Simulation of Radar Systems, IEE Colloquium on*, pages 11/1–11/4, Feb 1993.

[6] https://www.nads-sc.uiowa.edu/sim_nads1.php. Access August 2015.

[7] Kareem Abdelgawad, Mohamed Mahmoud Abdelfahim Abdelkarim, Bassem Hassan, Michael Grafe, and Iris Gräßler. A scalable framework for advanced driver assistance systems simulation. In *SIMUL2014 (IARIA)*, 6th International Conference on Advances in System Simulation (SIMUL 2014). International Academy, Research, and Industry Association (IARIA), October 2014. Nice, France.

[8] Sebastian Hafner. Echtzeitsimulation von adas-sensoren. *Hanser automotive*, 2015.

[9] Z. Magosi D. Lindvai-Soos A. Eichberger, S. Bernsteiner. Integration of a phenomenological radar sensor modell in ipg carmaker fpr simulation of acc and aeb systems. 2014.

[10] Roy Bours Robin Schubert, Norman Mattern. Simulation von sensorfehlern zur evaluierung von fahrerassistenzsystemen. *ATZelektronik*, 2014.

[11] B.R. Mahafza and A. Elsherbeni. *MATLAB Simulations for Radar Systems Design.* CRC Press, 2003.

[12] Clive Alabaster. *Pulse Doppler radar.* The Institution of Engineering and Technology, Stevenage, 2012.

[13] J. Toomay and P.J. Hannen. *Radar Principles for the NonSpecialist, 3rd Edition.* Electromagnetics and Radar Series. Institution of Engineering and Technology, 2004.

[14] W.L. Stutzman and G.A. Thiele. *Antenna Theory and Design.* Antenna Theory and Design. Wiley, 2012.

[15] D.J. Griffiths. *Elektrodynamik*. Always learning. Pearson Studium, 2011.

[16] Electromagnetic radiation and polarization. Access August 2015.

[17] Robert M. O'Donnell. Radar systems engineering ,lecture 4,the radar equation. 2010.

[18] Merrill I. Skolnik. *Radar Handbook*. McGraw-Hill, 1990.

[19] Oliver Günther. *Modellierung und Leakage-Kompensation von 77GHz FMCW-Weitbereichsradar-Transceivern in SiGe-Technologie für Kfz-Anwendungen*. PhD thesis, Technische Universität Erlangen-Nürnberg, 2008.

[20] Guido Joormann. Einrichtung eines antennenmesssystems für sogenannte fernfeldmessungen. Technical report, Universität Duisburg-Essen.

[21] H. Winner, S. Hakuli, F. Lotz, and C. Singer. *Handbuch Fahrerassistenzsysteme: Grundlagen, Komponenten und Systeme für aktive Sicherheit und Komfort*. ATZ/MTZ-Fachbuch. Springer Fachmedien Wiesbaden, 2015.

[22] P.E. Pace. *Detecting and Classifying Low Probability of Intercept Radar*. Artech House radar library. Artech House, 2009.

[23] S. Schelkshorn. *Multisensorielle Positionsbestimmung aus Dopplersignalen*. Logos-Verlag, 2008.

[24] Zoltan Magosi. Modellbildung und simulation eines radarsenosors für die virtuelle entwicklung von fahrerassistenzsystemen. Master's thesis, Technische Universität Graz, 2013.

[25] U. Lübbert. *Target Position Estimation with a Continuous Wave Radar Network*. Cuvillier, 2005.

[26] Florian Fölster. *Erfassung ausgedehnter Objekte durch ein Automobil-Radar*. PhD thesis, Technischen Universität Hamburg, 2006.

[27] William P. Delaney Willam E. Courtney Alan J. Fenn, Donald H. Temme. The development of phased-array radar technology. *Volume*, 2000.